Author Preprint Version – Paper published by Elsevier as:
T. Gernay, N. Elhami Khorasani, M. Garlock, Engineering Structures 113 (2016), pp. 259-276

Fire Fragility Curves for Steel Buildings in a Community Context: A Methodology

Thomas Gernay[a,1,*], Negar Elhami Khorasani[a], Maria Garlock[a]

[a]Dept. of Civil and Environmental Engineering, Princeton University, Princeton, NJ, U.S.A.
thomas.gernay@ulg.ac.be, nelhami@princeton.edu, mgarlock@princeton.edu

Highlights

- We propose a methodology for developing fire fragility functions for buildings
- The methodology is applied to a prototype multi-story steel building
- Uncertainties in fire, thermal, and structural models are considered in the analysis
- Event tree is used to combine fire scenarios in different building locations
- The functions allow for damage loss assessment due to fire in a community context

Abstract

This paper proposes a novel methodology for developing fire fragility functions for an entire steel building - meaning that the function is not specific to a location within the building. The aim is to characterize the probabilistic vulnerability of steel buildings to fire in the context of community resilience assessment. In developing the fragility functions, uncertainties in the fire model, the heat transfer model and the thermo-mechanical response are considered. In addition several fire scenarios at different locations in the building are studied. Monte Carlo Simulations and Latin Hypercube Sampling are used to generate the probability distributions of demand placed on the members and structural capacity relative to selected damage thresholds. By assessing demand and capacity in the temperature domain, the thermal and the structural problems can be treated separately to improve the efficiency of the probabilistic analysis. After the probability distributions are obtained for demand and capacity, the fragility functions can be obtained by convolution of the distributions. Finally, event tree analysis is used to combine the functions associated with fire scenarios in different building locations. The developed fire fragility functions yield the probability of exceedance of predefined damage states as a function of the fire load in the building. The methodology is illustrated on an example consisting in a prototype nine-story steel building based on the SAC project.

Keywords: Fire; Fragility Analysis; Steel Building; Structural Reliability; Urban Resilience; Community Risk Assessment

http://dx.doi.org/10.1016/j.engstruct.2016.01.043

[1]Permanent address: Structural Engineering Department, University of Liege, Quartier Polytech 1, allee de la Decouverte 9, 4000 Liege, Belgium. thomas.gernay@ulg.ac.be

1. Introduction

In recent years, the methods for analyzing structures in fire have moved towards a probabilistic framework. This framework explicitly recognizes the role of uncertainty in the evaluation of the response of structural systems to fire exposure. Hence, it provides valuable information about the reliability of structural systems, which is not accessible with deterministic methods. The reliability of structures in fire is an essential component of a safer and more resilient built environment.

In this shift towards probabilistic analysis, research efforts have notably focused on developing probabilistic models for the fire engineering parameters with significant uncertainty. Iqbal et al. computed the statistical parameters based on raw experimental data for parameters such as the compartment characteristics and thermal properties of fire protection material [1]. Elhami Khorasani et al. conducted an extensive survey data on fire load density in office buildings and proposed a probabilistic model based on a Bayesian approach [2]. Statistics have also been reported for the mechanical loads [3, 4] and for the evolution of the mechanical properties of steel with temperature [5]. Additionally, research has progressed towards providing the probabilistic methods to account for these uncertainties in fire engineering. Lange et al. [6] established a methodology for performance-based fire engineering of structures based on the performance-based earthquake engineering framework developed in the Pacific Earthquake Engineering Research (PEER) Center. Nigro et al. conducted a probabilistic plastic limit analysis of a steel-braced parking structure using Monte Carlo simulation [7]. Guo and Jeffers [8] provided a comparison between the first/second order reliability methods and Monte Carlo approach for the reliability analysis of a protected steel member in fire. The methods proposed so far have mainly focused on the fire reliability of isolated structural members rather than structural systems [9-12]. Additional research is needed to develop a more comprehensive framework that incorporates the uncertainties in fire scenario, heat transfer processes and thermo-mechanical response in a global methodology at the building scale.

In seismic engineering, the research community has developed a probabilistic framework to evaluate the vulnerability of the built environment to earthquake hazard. In order to assess the damage loss in a community of buildings subjected to a given earthquake, fragility functions have been developed for the different typologies of structures, e.g. [13-15]. These functions relate the probability of exceeding certain levels of damage in a structure with the intensity of the hazard affecting the structure. They incorporate the uncertainties on the demand and the capacity affecting the structural response. For an earthquake, the hazard intensity for a building can be measured by, for instance, the peak ground acceleration or spectral displacement.

In fire engineering, the only research works focused on fragility functions, to the authors' knowledge, are due to Vaidogas et al., who developed fragility functions for timber members in fire with the char depth as the intensity measure [16]. The framework established by Lange et al. [6] for performance-based fire engineering, based on the PEER methodology, uses fragility functions in order to estimate the damage measures based on the engineering demand parameters. The pioneering contribution of Lange et al. addresses important questions such as the selection of the intensity measure and the link between the hazard and the structural domains, which provides insight for the present research. The difference in approach between

the former contributions and the authors' is that the former use fragility functions at the member level while the authors use the fragility functions in a system level approach to quantify vulnerability of a structure.

Fragility functions offer a comprehensive method for characterizing the vulnerability of structures to specific hazards, while incorporating explicitly the effects of uncertainties. The fragility functions can be plotted to convey visually the effects of the uncertain parameters on the vulnerability; the graphs of the functions are referred to as fragility curves. Hence, this method is convenient for conducting sensitivity analyses or comparing different typologies of structures as regards the vulnerability to fire. Additionally, this approach is well adapted to the issue of community resilience against man-made or natural hazards. The latter reason explains the popularity of this approach in seismic engineering. Yet, the concern about the resilience of a community of buildings extends to fire hazard. For instance, conflagrations affecting a community may occur following a major earthquake, as highlighted by past events such as the Loma Prieta earthquake in 1989 [17-18]. In this case, fire fragility functions are needed for the different typologies of buildings in the community to evaluate the damage loss due to fire.

In future, fire fragility functions could be used as a tool for evaluating a city's resilience to fire hazard. The functions are intended to be incorporated into a broader framework in conjunction with Geographic Information System (GIS) software. For instance, the software HAZUS developed by FEMA incorporates seismic fragility functions; it could be enriched with fire fragility functions. In this framework, the functions could be used in conjunction with data on infrastructure and the built environment as well as probabilistic models for the occurrence and spatial distribution of ignitions. By combining the probability of occurrence of fire with the fire fragility functions, the user could estimate the structural damage within a community. Possible applications include the prediction of the extent of probable losses due to fire within a certain time frame (e.g. per year) or following a specific event such as an earthquake or an explosion in an industrial area. Such probabilistic predictions will provide input for risk-informed decision making at the scale of a community.

Based on these considerations, this research proposes a methodology for developing fire fragility functions for steel buildings. The contribution of this work is twofold. First, the novel methodology provides a comprehensive framework for probabilistic fire analysis, by addressing the different sources of uncertainties (fire scenario, heat transfer processes, thermo-mechanical response) at the level of the structural system (the entire building). Second, fire fragility functions developed following this methodology could be used in the probabilistic assessment of a community response to a fire hazard. In future research, fire fragility functions will be derived and implemented into a GIS based risk assessment software platform. Using such a platform, one will then be able to assess the expected risk and cost associated with fire events (e.g., fire following earthquake) for a community of buildings.

The general procedure for the development of fire fragility functions for community resilience assessment is illustrated in Figure 1.

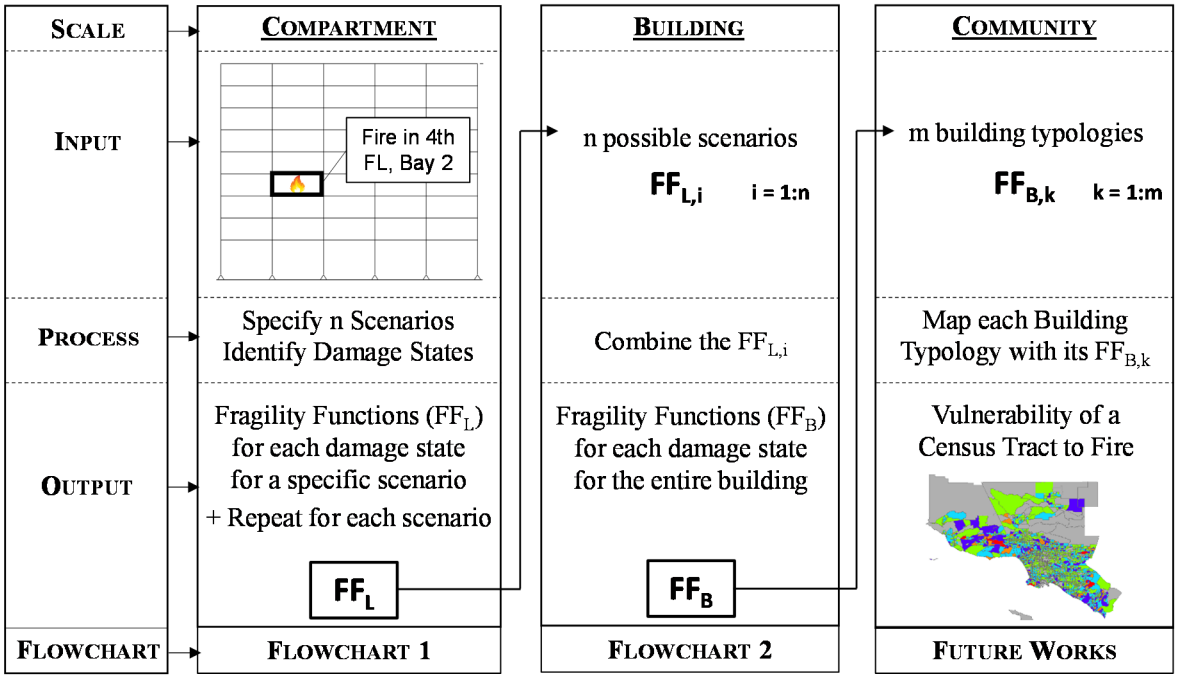

Figure 1. Development of fire fragility functions for community resilience assessment.

The procedure in Figure 1 deals with different scales. At the local scale, the local fragility functions, FF_L, are derived considering that the fire develops in a well-defined compartment of the building. These fragility functions will generally be different for each fire location within a same building, i.e., $FF_{L,i} \neq FF_{L,j}$. In this work, it is assumed that the fire remains contained within one compartment. The possibility of fire spread beyond a compartment will be addressed in future works. At the scale of the building, the many local fragility functions (corresponding to each fire location) must be combined in order to yield the building fragility functions, FF_B. The latter characterize the overall vulnerability of the building to fire. Finally, at the scale of the community, these building fragility functions are mapped to the buildings of the same typology. Other typologies of buildings need their own fragility functions. Hence, the resilience assessment of a community requires the inventory of the buildings in this community with their typologies (structural types) and the fragility functions $FF_{B,k}$ associated to each typology. The methodology for generating the fragility functions at the local scale and at the building scale is described in the next section. The extension at the community level will be addressed in future works. The "Flowchart" described in Figure 1 refers the reader to flowcharts presented in next sections of this paper.

This paper is structured as follows. Section 2 describes the proposed methodology for developing fire fragility functions. A framework is presented to construct the fragility functions at the scale of a compartment and then to combine them at the scale of a building. Section 3 introduces a prototype building that is used as a worked example. This example is intended for illustration of the methodology and requires the adoption of simplifying assumptions; it should be considered as an introduction to possible future applications. Section 4 discusses the parameters with uncertainty in the worked example. Section 5 addresses the probabilistic assessment of capacity of the structure in fire, whereas Section 6 addresses the probabilistic assessment of the demand placed on the structure. In Section 7, the methodology for

constructing the fire fragility functions is applied to the worked example, using the results of Section 5 and 6. The vulnerability of the prototype building to fire is obtained and the results are discussed. Finally, the conclusions of this research are presented in Section 8.

2. Methodology for developing Fire Fragility Functions

Fire fragility is a conditional probability statement describing the vulnerability of a system subjected to a given fire intensity. When developing fire fragility functions, it is assumed that a fire that is able to endanger the structure has started; such fire is referred to as structurally significant fire in this work. Hence, the factors that influence the probability of a structurally significant fire to happen, such as the presence of fire detection or sprinkler systems, have no effect on the fragility functions.

A methodology for generating analytical fire fragility functions is developed in this paper. For the sake of clarity, the methodology is presented in the framework of a practical example, namely a nine-story steel frame building. The example is intended as an introduction to possible applications, using a series of simplifying assumptions. The proposed methodology can be used with other steel structures in fire.

The final objective of the methodology is to obtain combined fragility functions representing the overall vulnerability of a building, independently of the fire location. This requires first to develop the Local Fragility Functions, $FF_{L,i}$, corresponding to the *n* possible fire scenarios (i.e., fire locations) that lead to different fragility functions. The adopted procedure is illustrated in Flowchart 1 (Figure 2) and explained in Section 2.1. Once the Local Fragility Functions are obtained, they can be combined to derive a single function per damage state, to represent the global vulnerability of the building. This is performed following the procedure illustrated in Flowchart 2 (Figure 5) and explained in Section 2.2.

2.1 Fire Fragility Functions corresponding to a specific fire location (Flowchart 1)

Flowchart 1 in Figure 2 illustrates the procedure to generate the fire fragility functions corresponding to a specific fire scenario, namely, to a fire developing in a compartment *i*.

The development of fragility functions requires the probabilistic assessment of the capacity of the structure, relative to predefined limit (or damage) states, and the probabilistic assessment of the demand placed on the structure, due to fire.

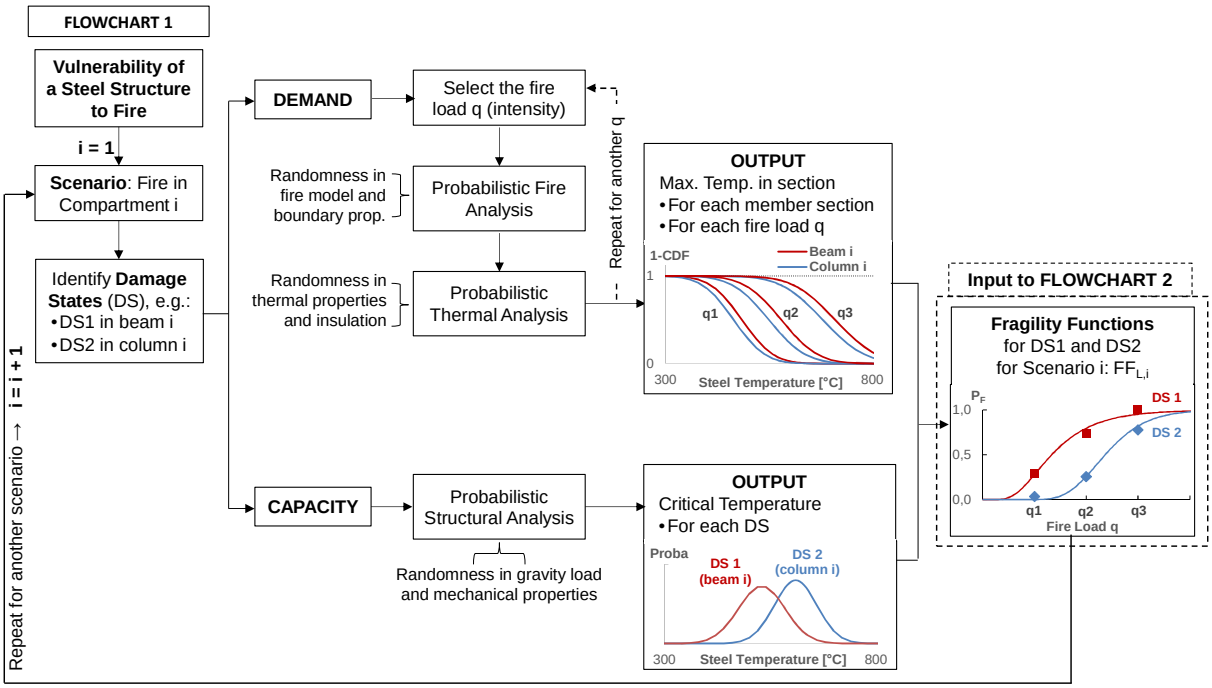

Figure 2. Flowchart 1: Procedure for the development of the Local Fragility Functions $FF_{L,i}$ corresponding to a fire located in compartment *i*.

2.1.1 Capacity Assessment

The first step focuses on the structural capacity. A realistic evaluation of the structural capacity in fire should take into account the variation in material properties with temperature and the fire-induced forces that build up in the structure as a result of differential thermal expansion. Due to the complexity of the interaction between the heated members and the surrounding structure, this evaluation may require advanced methods such as finite element method.

For structural steel members in fire, the exceedance of predefined damage states can be assumed to depend on the exceedance of a certain temperature in the section, referred to as the critical temperature. This concept of critical temperature is convenient because it allows defining the structural capacity independently of the thermal parameters. It postulates that the physics of the fire and the heat transfer processes do not influence the temperature at which the steel member reaches its damage state. These parameters do influence the time to reach the critical temperature, but the fragility functions derived in this research are not in the time domain. The verification of the resistance of a structural steel member in the temperature domain is a common approach in deterministic or semi-probabilistic design, for instance prescribed in Eurocode 3 [19]. This verification consists in comparing the temperature reached in the section with the critical temperature. As long as the temperature in the section (demand) remains lower than the critical temperature (capacity), the structural steel member is safe, see Figure 3a. Note that the critical temperature approach ignores the cooling phase. Therefore, damage states specific to the cooling phase (such as tension failure in the connections) are not considered in this work.

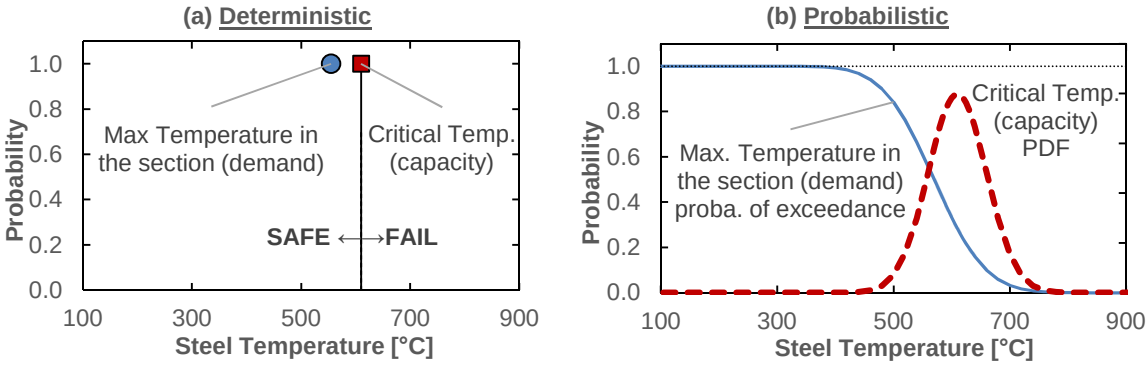

Figure 3. Reliability of a steel member in fire, assessed in the temperature domain: deterministic (a) versus probabilistic (b).

This approach can be extended to a probabilistic framework. Hence, the capacity with respect to a predefined damage state is expressed as a probability density function (PDF) of the exceedance of this damage state as a function of the steel temperature in the section (Figure 3b). Randomness in the structural parameters, for instance the mechanical properties at high temperature, are incorporated in this analysis. In this way, the concept of critical temperature is kept and extended to include the uncertainties and variability that affect the structural response. It offers the benefit that the structural capacity is defined without requiring any information about the demand, namely the fire. Therefore, the structural analysis is decoupled from the fire and heat transfer analyses in the Flowchart (Figure 2). The validation of this approach for the specific structure studied in this work will be presented in Section 5.3.

2.1.2 Demand Assessment

The second step deals with the demand placed on the structure. First, a physical variable must be chosen to represent the intensity measure of the hazard to which the vulnerability is assessed. In earthquake engineering, the hazard is usually characterized in terms of acceleration *g*. The development of fragility functions is thus conducted considering different levels of acceleration, to cover the range of possible earthquake scenarios. For structures in fire, the parameter that is best adapted to characterize the hazard (i.e. the fire) could be the fire load in a compartment (in MJ/m² of floor area). Indeed, the fire load is one of the main parameters affecting the intensity of a fire [2]. It may vary in a significant range and it has a straightforward definition that is easily understood by the different stakeholders involved in fire safety. Hence, it seems reasonable to develop fragility functions for structures in fire using the fire load as the intensity measure. In adopting the fire load as the intensity measure, it is conservatively assumed that oxygen will always be available in the compartment to support the fire growth and spread.

Regarding the demand assessment, fire and thermal (heat transfer) analyses are conducted in order to assess the distribution of the maximum steel temperature reached in the sections of the structural members. These analyses are conducted for a given level of the fire intensity measure, i.e. the fire load in the compartment. Uncertainties affecting the demand, such as the thermal properties of the materials, are included in the analysis. The output of the analyses is

thus a probabilistic distribution of the maximum temperature reached in the steel sections, for a given fire load. The result is presented in the form of a complementary cumulative distribution function (CDF) of the maximum steel temperature in the considered section (Figure 3b).

2.1.3 Fragility Functions

Using the outputs of the capacity and demand assessments, the fragility functions can be built (Figure 2). Convolution of the complementary CDF of demand with the PDF of the capacity relative to a given damage state gives the probability of reaching the damage state [15], i.e. the associated probability of "failure", see the following equation:

$$P_{F|H_{fi}} = \int_0^\infty \left[1 - F_{D|H_{fi}}(\alpha)\right] f_C(\alpha) d\alpha \qquad \text{Eq. 1}$$

In this equation, $P_{F|H_{fi}}$ is the probability of failure conditional to the occurrence of a fire H_{fi}; the demand D and capacity C are random variables characterized by their probability density functions $f_D(\cdot)$ and $f_C(\cdot)$; and $F_{D|H_{fi}}$ is the CDF of the demand relative to the fire H_{fi}. The issue lies in the evaluation of the probability laws for C and D, i.e. the capacity and demand assessment; this is the objective of Sections 5 and 6 of this paper. The solution of Eq. 1 is illustrated in Figure 4.

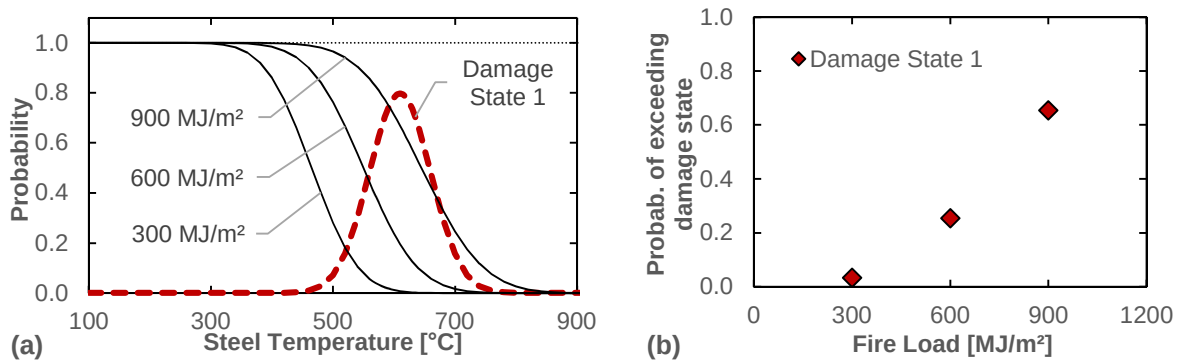

Figure 4. Convolution of PDF of damage state and complementary CDF of demand (a) leads to the derivation of the fragility points (b) for fire loads of 300, 600 and 900 MJ/m².

As shown in Figure 4, Eq. 1 yields a scalar: the probability of failure relative to a predefined damage state, given the fire intensity level (fire load) that was considered in the assessment of the demand placed on the structure. This procedure must be repeated for different levels of intensity measure. By varying the fire load and repeating the procedure, different points relating the fire load and the probability of failure are obtained.

The fragility functions are then built to fit these points assuming a lognormal distribution. The use of a lognormal probability density function for fitting of the fragility points is an assumption often adopted for fragility functions, e.g. in [13] and [15].

2.1.4 Advantages and Limitations of the Methodology

The proposed methodology, based on the subdivision in a thermal part (demand assessment) and a structural part (capacity assessment), presents several advantages over a more straightforward approach consisting in analyzing the complete system (thermal and structural) a large number of times. In a straightforward approach, for a given fire load, one would perform a complete thermal and structural analysis for each set of values of the uncertain parameters. A large number of realizations would be required to assess the probability of failure for a given fire load, due to the high dimensionality of the system, which includes uncertain parameters affecting significantly the thermal response (e.g. thermal properties of the insulation) and the mechanical response (e.g. gravity loads). In contrast, the proposed methodology recognizes that the only influence that the thermal subsystem has on the structural subsystem is the steel temperature. Hence, it is more efficient to divide the system in two subsystems of lower dimensionality, namely a thermal subsystem and a structural subsystem, with the steel temperature as the connecting link between them. The advantages of the proposed methodology over a straightforward approach are the following:

- It leads to a significant reduction of the number of realizations required to have a statistically converged estimation of the probability of failure.
- It allows using theoretical models and methods of varying levels of complexity for assessing the demand (thermal part) and the capacity (structural part). For instance, assessing the capacity of a structure in fire may require Finite Element (FE) modeling, which is complex and computationally demanding. However, the thermal analyses of the sections that compose the structure can often be performed using simple analytical models. Owing to the decoupling between the two tasks, full advantage can be taken of these analytical models to assess the CDF of the demand on the system.
- In case of a change in the design of the structure, it reduces the number of simulations that have to be repeated for updating the system reliability. For instance, if the thickness of the thermal protection on the steel sections has to be increased due to a change in the fire resistance requirement, it only affects the CDF of the demand placed on the system, i.e. the maximum steel temperature reached in the section. It has no effect on the structural capacity. Consequently, the system reliability update requires to perform again the demand assessment, but not the capacity assessment (structural analysis). In a straightforward approach, this change in design would imply to repeat all the analyses from the beginning.

In contrast, the methodology relies on a few simplifying assumptions that should be taken into account when extending the procedure to other building types:

- As the capacity is assumed independent of the heating rate, it is assumed that the stress-strain material behavior does not depend on time. For steel, it means that creep is not given explicit consideration. This is in line with the recommendation of Eurocode 3 [19] for heating rates between 2 and 50 K/min.
- Having the capacity independent of the heating rate, it is assumed that the thermal gradient in the section does not affect the capacity. This is a simplifying assumption that is reasonable for protected steel members, in which the thermal inertia of the insulation

smoothens the gradient in the steel. However, its validity is not ensured for all types of buildings.

- This methodology does not address the structural response in cooling phase.

2.2 Combined Fire Fragility Functions for the entire building (Flowchart 2)

Flowchart 2 in Figure 5 illustrates the procedure for combining the $FF_{L,i}$ corresponding to the different fire locations into a single Combined Fragility Function FF_B per damage state to characterize the overall building vulnerability.

The Local Fragility Functions $FF_{L,i}$ are characterized by their probabilistic parameters, mean and standard deviation. These parameters are used to evaluate the probabilistic parameters of the combined functions: q_c (median) and ζ_c (standard deviation of the lognormal distribution).

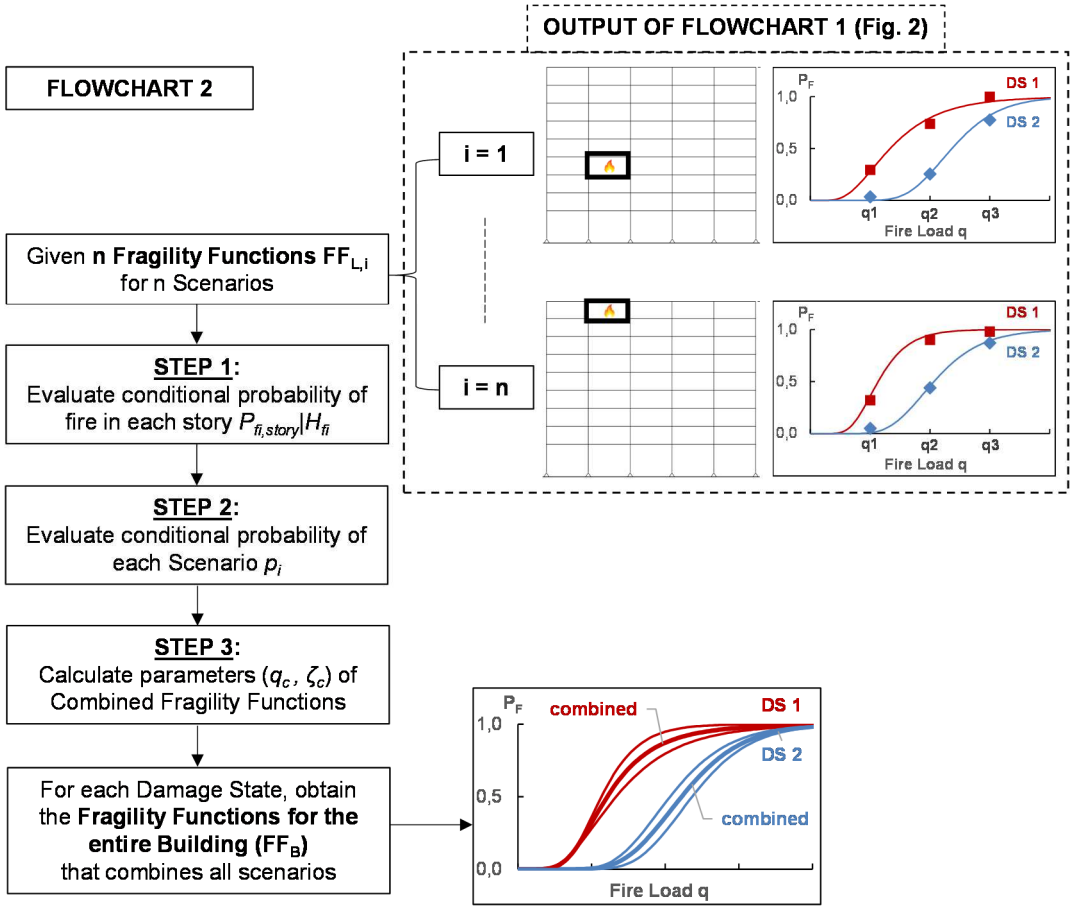

Figure 5. Flowchart 2: Procedure for the combination of the Local Fragility Functions $FF_{L,i}$ into the combined fragility functions FF_B for the global vulnerability of the building.

However, the conditional probability of each scenario *i* associated with the function $FF_{L,i}$ must first be assessed. These conditional probabilities are used to weigh the parameters of the corresponding scenario in the calculation of the parameters q_c and ζ_c for the entire building. The scenario *i* refers to a fire occurring in compartment *i*. It is thus required to evaluate the respective likelihood of having a fire in each of the compartments, given a fire starts in the building. This

evaluation is conducted in two steps: the allocation of probabilities is first conducted between stories (step 1) and then between compartments (step 2), see Figure 5. The procedure is explained in details and applied to the prototype building in Section 7.2.

3. Prototype Steel Building

3.1 Geometry and Design

The considered building prototype consists of a nine-story steel building designed in accordance with the FEMA/SAC project, for the Los Angeles model building. The building is 45.72 m by 45.72 m in plan, consisting of five bays of 9.144 m (30 ft) in the two directions. The structure is composed of four moment resisting frames on the perimeter, and four interior gravity frames, see Figure 6. When laterally loaded (wind, earthquake), the interior frames lean against the perimeter frames, the latter ensuring the in-plane stability of the building. The columns of the interior frames are continuous on the nine-story but the beams have pinned connections (statically determinate beams). The total height of the building is 37.182 m, divided between a 1st floor of 5.486 m (18 ft) high and the 8 other floors of 3.962 m (13 ft) high. The fire compartmentation of the building is assumed to be based on a subdivision in compartments of 9.144 m long and 6.096 m wide, hence a surface area of 55.74 m² per fire compartment.

The perimeter frames, designed for seismic resistance, are made of relatively heavy protected steel sections. Owing to their large thermal massivity (i.e. ratio of cross-section area to perimeter), they are not likely to be affected significantly by a fire, and this has been confirmed by a previous study [20]. In contrast, gravity frames have a lower massivity and a higher utilization ratio, so they are most likely to reach their critical temperatures first [21]. As a consequence, this work focuses on the effects of the fire on the gravity frames only.

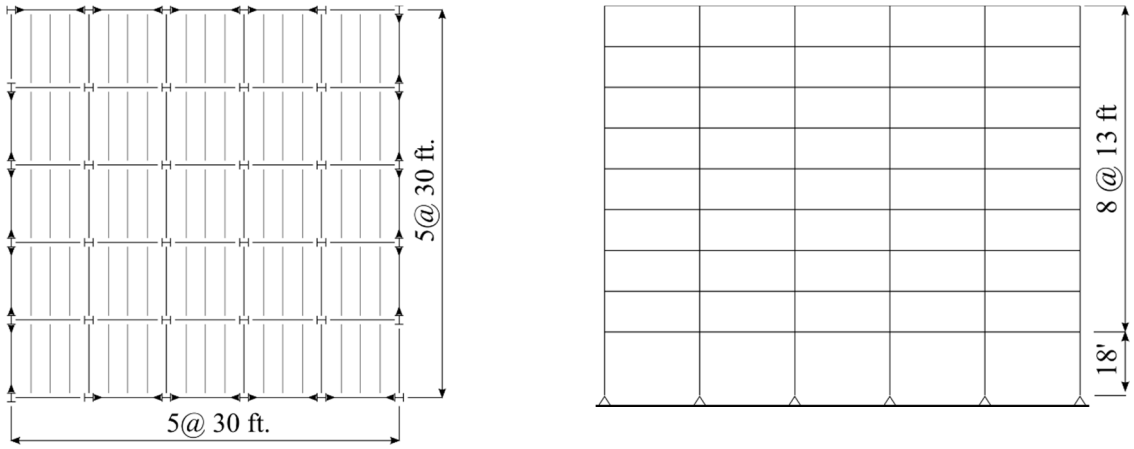

Figure 6. 9-story steel building: plan view (left) and elevation view of a gravity frame (right).

The sections of the beams and columns for the interior frame are given in Table 1. The columns sections range from W14x43 to W14x109. Note that, in contrast, the moment frame columns sections range from W14x342 to W14x665. The slab is 102 mm average depth in concrete with siliceous aggregates. The steel sections (beams and columns) are protected with

a sprayed fire-resistive material (SFRM) of nominal thickness 39 mm. The unfactored gravity loads distributed on the interior beams are given in Table 1. The nominal values of the steel yield strength and Young modulus are 345 MPa and 200,000 MPa, respectively. The concrete compressive strength is 28 MPa.

Table 1. Sections of the structural members and (unfactored) gravity loads.

Level	Interior Beam	Interior Column	Distributed Loads [kN/m]		
			Dead Load	Live Load	Partitions
9	W18x40	W14x43	43.72	5.25	3.96
7-8	W21x44	W14x53	41.88	13.21	3.96
5-6	W21x44	W14x68	41.88	13.21	3.96
3-4	W21x44	W14x82	41.88	13.21	3.96
1-2	W21x44	W14x109	41.88	13.21	3.96

3.2 Numerical Model

The building has been modeled in the non-linear finite element software SAFIR [22] developed at University of Liege for the analysis of the behavior of building structures in fire. SAFIR allows conducting a thermal analysis of the sections of the structural members, followed by a structural analysis of the building that takes into account the results of the thermal analysis. Here, the response of one interior frame is studied in its plane, meaning that the model is built in two dimensions. First, a two-dimensional thermal FE analysis is conducted for each heated member (beams and columns) using cross-sections that are discretized in fibers. The modeling of the beam section includes a 2.3 m effective width of concrete slab, i.e. one quarter of the span, see Figure 7a. Then, a structural analysis is performed using three-noded, two-dimensional beam elements. In a fiber analysis, at every point of integration, all variables such as temperature, strain, stress, etc. are uniform in each fiber. The time-temperature evolution in each fiber results from the previously conducted thermal analysis. The structural analysis takes into account geometrical and material non-linearity, including large deflections. Global instabilities (buckling) are also accounted for, but local buckling cannot be represented with the beam finite elements. Thermal expansion is included in the analysis and therefore fire-induced forces are considered in the structure. The composite effect of the concrete slab is taken into account in the structural analysis assuming a full transfer of horizontal shear at the steel-concrete interface. Connections are not represented in the model; hence it is implicitly assumed that member failure occurs prior to connection failure.

The lateral in-plane stability of the interior frames is provided by the parallel moment resisting perimeter frames, owing to the concrete slab that plays the role of a diaphragm. The concrete slab transmits in-plane horizontal forces, allowing two parallel frames to work together. This means that the horizontal displacements at the top of each interior frame column are linked to the horizontal displacements at the top of each corresponding perimeter frame column. To capture this effect in the 2D numerical model, one moment resisting perimeter frame is modeled next to the studied interior frame (in the same plane, as it is a 2D model). Then, the horizontal displacements are set to be equal at the top of each corresponding columns in the two frames (e.g. the top node at the second story of the third column of the interior frame

has the same horizontal displacement as the top node at the second story of the third column of the perimeter frame). However, this condition is not applied to the compartment where the fire develops, due to the cracking of the concrete slab in this compartment [23]. As a result, the interior frame transmits horizontal forces, which build up due to the fire and to second order effects, to the perimeter frame. These horizontal forces create moments that are eventually balanced by the reactions at the base of the perimeter frame columns.

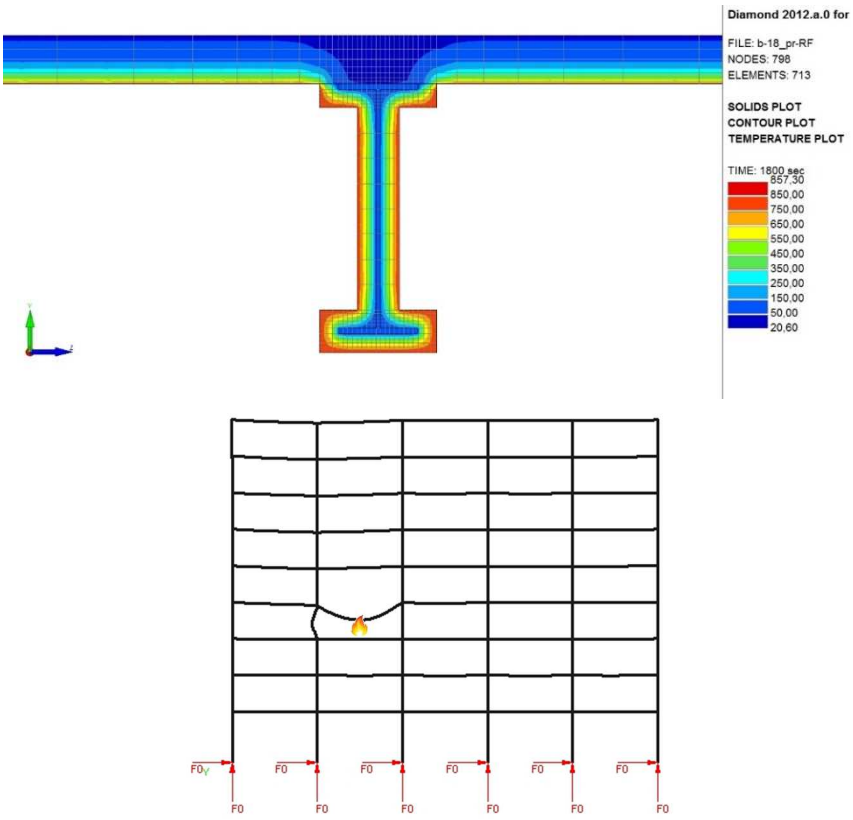

Figure 7. (a) Thermal analysis of the protected beam (b) 2D FE model of the building.

The stress-strain relationship for steel at high temperature is adopted from Eurocode 3 [19] and the relationship for concrete is taken from [24]. However, the evolution of steel yield strength and Young modulus with temperature is not taken from Eurocode but it is evaluated using probabilistic models, to account for the uncertainties in these parameters, as discussed in the next section.

Figure 7b presents the structural model of the interior frame, with the deflected shape at collapse (amplified two times) for a fire in the second bay of the fourth floor. The deflections are mainly limited to the fire-exposed compartment. The high temperatures in the fire-exposed elements lead to additional forces in the surrounding elements, but these fire-induced forces do not lead to any significant lateral displacement of the structure (no sway effect). This is due to the lateral restraint provided by the perimeter moment resisting frames, connected to the interior frame through the slabs.

4. Parameters with Uncertainty

In order to evaluate the structural reliability in fire, the many uncertainties associated with the performance of the system need to be considered explicitly in the calculation. The demand on the system depends on random parameters affecting the fire development, such as the ignition location, the fire load and the characteristics of the compartment. It is also influenced by random parameters governing the heat transfer process, such as the thermal properties of the materials. Similarly, the capacity of the system depends on parameters that exhibit inherent randomness, such as the mechanical properties of the materials or the gravity loads.

Clearly, it is neither practical nor relevant to consider all possible configurations and sources of uncertainties. Based on literature and engineering judgment, only the most significant sources of uncertainties are selected, considering a trade-off between computational efficiency and accuracy. Table 2 summarizes the parameters used in this study and indicates which parameters have sources of uncertainty.

Table 2. Parameters for the fire model, the heat transfer model and the mechanical model (data partially adopted from [8, 25]).

Parameter		**Units**	**Distribution**	**Mean value**	**COV**
(1) Scenario	Fire in compartment i	-	See Section 7.2		-
(2) Fire model	Fire load q	[MJ/m²]	Intensity measure	100-2000	-
	Opening factor O	[$m^{1/2}$]	Deterministic	0.0424	NA
	Surface ratio A_f/A_t	-	Deterministic	0.2535	NA
	Thermal inertia b	[J/m²$s^{1/2}$K]	Deterministic	762	NA
(3) Heat Transfer					
Properties of SFRM	Thickness d_p	[m]	Lognormal	Nominal+1.6mm	0.2
	Conductivity k_p	[W/mK]	Normal Stand.	See Table 3	-
	Density ρ_p	[kg/m³]	Deterministic	See Table 3	NA
	Specific heat c_p	[J/kgK]	Deterministic	See Table 3	NA
Properties of Steel	Density ρ_a	[kg/m³]	Deterministic	from EC3 [19]	NA
	Specific heat c_a	[J/kgK]	Deterministic	from EC3 [19]	NA
Geometric properties	Area A_p	[m²/m]	Deterministic	vary with section	NA
	Volume V	[m³/m]	Deterministic	vary with section	NA
(4) Structural Model					
Properties of Steel	Yield strength $f_{y,\theta}$	[N/m²]	Normal Stand.	See Table 3	-
	Young modulus E_θ	[N/m²K]	Normal Stand.	See Table 3	-
Load	Dead load	[N]	Normal	1.05xNominal	0.1
	Live load	[N]	Gamma	0.24xNominal	0.6
	A factor	-	Normal	1	0.04
	B factor	-	Normal	1	0.2
	E factor	-	Normal	1	0.05

4.1 Scenario

The vulnerability of the building will depend on the location of the compartment in which a fire develops. In the adopted compartment fire assumption, the fire actions are assumed to remain contained within the compartment in which the fire started. The location of the fire is associated with a large variance, since a fire is approximately as likely to occur in any of the compartments of the building (the method to estimate the distribution of fire events among the

compartments is presented in details in Section 7.2). Meanwhile, the fire location has a major influence on the structure response since, for instance, the sections of the structural members and the gravity loads supported by the columns vary among the compartments. As a result, the different possible fire locations should necessarily be considered in the analysis.

In the considered building, the sections of the structural members and the gravity loads vary with the story, see Table 1. Consequently, at least one compartment fire per story must be analyzed, i.e. nine scenarios. The compartments of the second bay are selected for the analyses. For the columns, the analysis of the nine compartments of the second bay is found to be representative of all other compartments. (Note that the perimeter columns are heavier sections, as they belong to moment resisting frame. Therefore, a fire in a perimeter bay still results in a failure of an interior column.) For the beams however, preliminary (deterministic) analyses show that the fire response is affected by the presence of surroundings bays, so that the beam capacity for an interior bay is different than for a perimeter bay. It results that one additional scenario per beam section type must be analyzed in a perimeter bay. Only two section types are used for the beams (Table 1). Therefore, two compartments of a perimeter bay must be analyzed. The first bay compartments on the fourth story and on the ninth story are selected to analyze the response of the two beam section types in perimeter bays. In total, eleven scenarios are thus considered, see Figure 8, and these eleven scenarios are representative of the entirety of the possible configurations. It results that n = 11 in Figure 1 and in the Flowchart 2 (Figure 5).

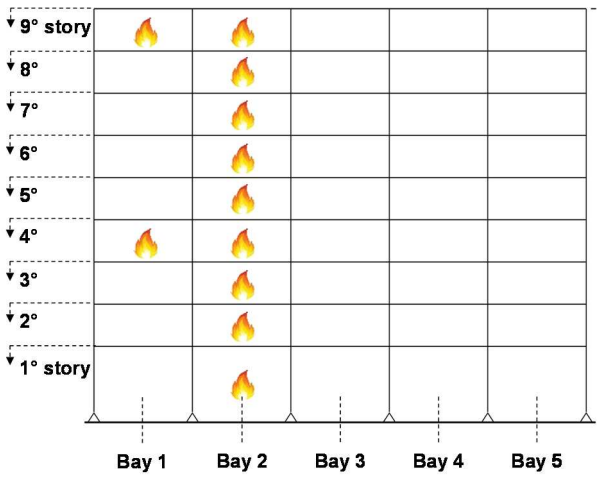

Figure 8. Eleven scenarios (i.e. fire locations) are successively studied; they are selected to cover the entirety of the possible configurations (member section type, gravity load, etc.).

4.2 Fire model

The building vulnerability is dependent on the time-temperature evolution of gas in the compartment. This fire model is influenced by the fire load, the geometry of the compartment and the thermal properties of the boundary of enclosure.

Fire load is the most important parameter characterizing a fire hazard. Several studies have shown its large variance and paramount influence on the structural reliability in fire [8, 20, 25].

Consequently, the fire load is taken as the intensity measure to characterize the vulnerability of a structure to fire hazard, as explained in Section 2. The analyses are conducted for several levels of fire load successively fixed between 100 and 2000 MJ/m², to cover the range of realistic fire loads in a building compartment. Hence, there is no need to adopt a probabilistic distribution for the fire load when constructing the fragility functions. Once the fragility functions have been constructed, the user can assume freely the distribution of fire load in the building under study, based on the usage and other features of this building, in order to determine the probable level of damage. This could be done for instance using the NFPA 557 standard [26] or Eurocode 1 [27] for fire loads in buildings.

The geometric properties of the compartment, which include the opening factor and the surface ratio, are assumed to be deterministic, based on a typical compartment of the prototype building. The values are given in Table 2.

The thermal properties of the boundary of enclosure are assumed deterministic, considering that the walls and ceiling of the prototype building are lined with gypsum plaster board. This assumption is conservative compared to concrete walls, because concrete walls have a higher thermal inertia than gypsum plaster boards. Therefore, the gas temperature in the compartment would be lower if concrete walls were used instead of gypsum plaster board. The properties for gypsum are taken from Drysdale [28]: conductivity k_g = 0.48 W/mK; specific heat c_g = 840 J/kgK; density ρ_g = 1440 kg/m³.

4.3 Heat transfer

The heat transfer processes govern the temperature increase in the sections of the structural members and, therefore, affect the building vulnerability. These processes depend on the thickness and thermal properties of the thermal insulating material, the thermal properties of steel and the geometry of the section.

Sensitivity analyses on the uncertain parameters affecting the heat transfer model for steel members protected with SFRM have shown the prevailing importance of the thickness and conductivity of SFRM [8]. These two parameters have a significant influence on the model (large sensitivity coefficients) in addition to being associated with large variances. As a result, the thickness and conductivity of SFRM are treated as random parameters in the model. For the SFRM thickness, a lognormal distribution is assumed with a mean value equal to the nominal value of 39 mm plus 1.6 mm and a coefficient of variation of 0.2 [25]. Regarding the SFRM conductivity, the probabilistic model from [5] is adopted, see Table 3.

On the other hand, the density and specific heat of SFRM can be treated as deterministic because of their lower sensitivity coefficients compared with conductivity. In the probabilistic equations of Table 3, the random variable with standard normal distribution, ε, is considered equal to zero for the parameters that are assumed deterministic.

Thermal properties of steel can be treated as deterministic due to their relatively low variances; the properties are taken from Eurocode [19].

Finally, the section factor, calculated from the area and volume of the member, is treated as deterministic due to the relatively low variance of the geometric parameters.

Table 3. Probabilistic equations for the thermal and mechanical parameters, adopted from [5].

Parameter	Probabilistic Equation
SFRM - k_p	$k_p = exp(-2.72 + 1.89 \times 10^{-3}T - 0.195 \times 10^{-6}T^2 + 0.209 \times \varepsilon)$
SFRM - ρ_p	$\rho_p = exp(-2.028 + 7.83 \times T^{-0.0065} + 0.122 \times \varepsilon)$
SFRM - c_p	$c_p = 1700 - exp(6.81 - 1.61 \times 10^{-3}T + 0.44 \times 10^{-6}T^2 + 0.213 \times \varepsilon)$
Steel - $k_{y,\theta}$	$k_{y,\theta} = \frac{1.7 \times exp[r_{logit} + 0.412 - 0.81 \times 10^{-3} \times T + 0.58 \times 10^{-6} \times T^{1.9} + 0.43 \times \varepsilon]}{1 + exp[r_{logit} + 0.412 - 0.81 \times 10^{-3} \times T + 0.58 \times 10^{-6} \times T^{1.9} + 0.43 \times \varepsilon]}$ with $r_{logit} = ln\frac{(k_{y,EN}+10^{-6})/1.7}{1-(k_{y,EN}+10^{-6})/1.7}$
Steel – $k_{E,\theta}$	$k_{E,\theta} = \frac{1.1 \times exp[2.54 - 2.69 \times 10^{-3} \times T - 2.83 \times 10^{-6} \times T^2 + 0.36 \times \varepsilon]}{1 + exp[2.54 - 2.69 \times 10^{-3} \times T - 2.83 \times 10^{-6} \times T^2 + 0.36 \times \varepsilon]}$
Load	$P = E(A\ P_{DL,fi} + B\ P_{LL,fi})$

4.4 Structural model

The structural response depends on the mechanical properties of steel at high temperature and on the applied gravity loads during the fire event. Randomness in the steel mechanical properties and in the gravity loads are considered. The reduction of the steel mechanical properties with temperature is taken from [5], see Table 3. The factors applied to the dead and live loads are respectively taken as 1.05 and 0.24 [25], noting that under natural fire exposure, the probability of the maximum live load to coincide with a fire accident is low [3]. Therefore, the part of the live load applied in combination with the fire action is the arbitrary point-in-time live load, in the sense of the sustained component of the live load which remains relatively constant within a particular occupancy [3]. A gamma distribution with a COV of 0.6 is assumed for the live load and a normal distribution with a COV of 0.1 for the dead load, based on [8]-[25]. Finally, the total gravity load effect P is taken as: $P = E\ (A\ P_{DL,fi} + B\ P_{LL,fi})$, in which $P_{DL,fi}$ = 1.05 x P_{DL} and $P_{LL,fi}$ = 0.24 x P_{LL} are respectively the factored (random) dead and live load in fire situation; A and B are random variables reflecting the uncertainties in the transformation in loads into load effects; and E is a random variable representing the uncertainties in structural analysis [25]. The distribution parameters for A, B and E are given in Table 2.

5. Capacity Assessment

5.1 Definition of Damage States for a Steel Frame Building

The definition of the structural damage states should rely on parameters that can be obtained from the structural analysis, such as the rate of displacement at mid-span of a member. For a steel frame building with beams with pinned connections, two structural damage states are considered, one relative to the beams and one relative to the columns (Figure 9):

- DS1: Maximum flexural resistance of the beam, when the flexural capacity of the beam is exceeded and the mid-span vertical deflection increases dramatically;

- DS2: Maximum resistance of the column, when the column fails with a sudden increase in transversal deflection, whether due to exceedance of the buckling resistance of the column or exceedance of the section plastic capacity under combined compression and bending.

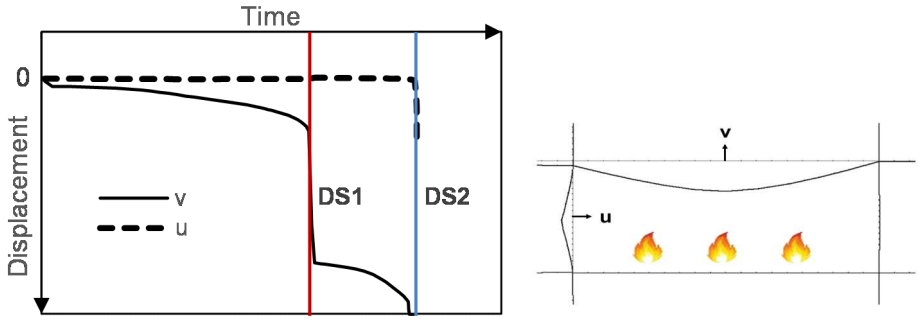

Figure 9. Damage states related to structural response, for a compartment fire in a steel frame building.

When the structure reaches the beam damage state (DS1), the bending moment in the beam drops suddenly while tensile axial forces build up in the steel beam, marking the sudden change from a bending mode to a catenary tensile action. This damage state corresponds to a local damage for the structure, characterized by major cracking of the concrete slab and beam mid-span deflections of the order of $1/10^{th}$ of the span. However, there is limited impact on the building functionality for the users. Provided that the end beam connections and the surrounding structure are able to sustain the tensile forces that built up in the beam as a result of the catenary action, the structure does not reach its ultimate capacity and the damage remains at the member scale. In three dimensions, a beneficial effect could also come from the development of tensile membrane forces in the plane of the concrete slab. Yet, this effect is not taken into account in the present analysis since it is computationally too expensive and previous research on numerical modeling of similar multi-story steel frame building in fire supports the validity of a two dimensional modeling approach [23].

The second damage state (DS2) corresponds to the failure of one of the frame columns. This state may coincide with the complete collapse of the structure, although in some cases, the redundancy and robustness of the structure may be sufficient to redistribute the forces after the loss of a column. The analysis of the progressive collapse mechanisms after the loss of one column is beyond the scope of the present work. However, the loss of one column may result in significant damage to the building, which will probably be beyond the point of repair and can be taken as a severe damage state.

In further analysis, non-structural damage states could also be identified in the building. For instance, it might be interesting to determine whether the integrity of non-structural elements is endangered by the fire. Non-structural elements such as compartment walls play a major role in the limitation of fire and smoke propagation. A reasonable assumption consists in linking the integrity of these non-structural elements with the response of structural elements, because significant deflections of the latter are likely to cause cracking, collapse or falling down of the former. Therefore, non-structural damage state could be identified by the attainment of a

deflection threshold in the structural members. However for practical application, the difficulty lies in defining a meaningful threshold, due to a lack of data and a variability in the connection design between non-structural and structural elements. In the example presented hereafter, no damage state related to the non-structural elements is taken into account, but this aspect will be considered in future works and it could be added in the methodology.

5.2 Deterministic Fire Resistance under ASTM E119 Fire

Before analyzing the effect of the many uncertainties on the system, it is useful to gain further insight into the fire behavior of the structure by conducting a deterministic analysis. As a case study, this section explores the fire resistance of the structure under standard fire exposure considering a fire in the compartment located on the second bay of the fourth floor. Similar analyses could be conducted for each of the compartments shown in Figure 8 but are not reported here since assessing the fire resistance of a simple frame structure is a well-established process. The standard fire that is considered is the ASTM E119 fire [29]. This fire is selected for the deterministic analysis because it is often adopted to evaluate the fire resistance rating of structural members. Nominal values, as defined in Section 3.1, are adopted for the parameters. The evolution of thermal and mechanical properties with temperature is based on the mean value of the probabilistic equations given in Section 4.

The FE analysis is performed with SAFIR using the 2D frame model described in Section 3.2. The analysis yields the evolution of displacements in the structure as a function of time. The vertical displacement at mid-span of the beam, and the transversal displacement at mid-height of the column, are plotted in Figure 10. The beam and column damage states are identified by the attainment of excessive rates of displacement, of the order of 50 mm/min. The beam damage state is reached after 111 minutes and the column damage state after 171 minutes. The temperature in the cross-section of each element (beam and column) is recorded at the time when the corresponding damage state is reached, see Figure 10. As the temperature is non-uniformly distributed in the elements, the average temperature is considered. This procedure yields the critical temperatures associated with the two structural damage states in the structure. This critical temperature is 527°C for the beam and 576°C for the column.

5.3 Validation of the Critical Temperature Approach

The time at which a structural damage state is reached depends, amongst others, on the physics of the fire (e.g. heating rate of the fire) and thermal properties of the structure (e.g. level of thermal protection). However, the temperature of the steel section when the damage state is reached is assumed to be independent of the fire and thermal properties. This assumption, which relates to the critical temperature concept for structural steel members, is verified here below. The structural capacity is studied by numerical simulation for a fire in the fourth floor and second bay compartment and assuming two different configurations. First, the sections of the structure are assumed to have no thermal protection, and the fire follows the standard ASTM E119 temperature-time curve. Second, the sections are protected with SFRM and subjected to

a natural fire (to be defined in Section 6). For each configuration, five simulations are run considering a set of random values for the mechanical parameters.

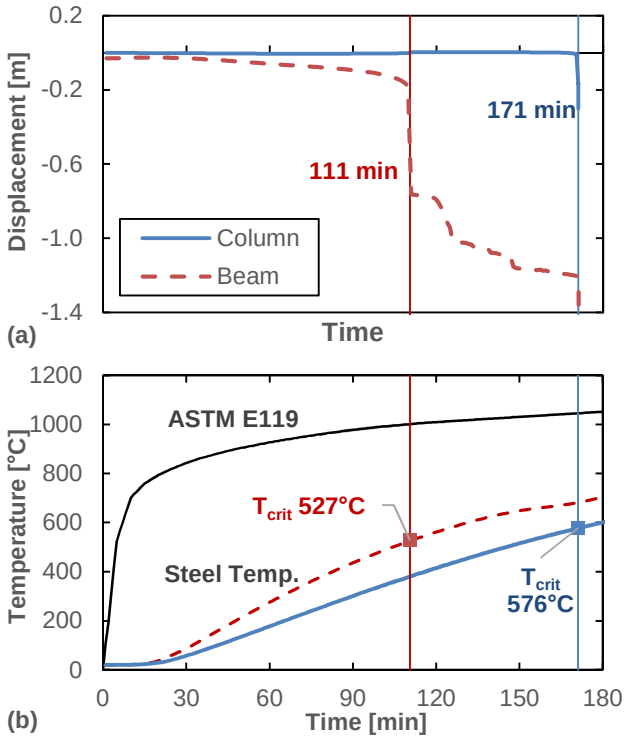

Figure 10. Evolution of vertical displacement at mid-span of the beam and transversal displacement at mid-height of the column (a); evolution of temperature in the sections (b).

For the two configurations, Figure 11a gives the time at which the column damage state is reached in the five simulations. In the time domain, the attainment of the column damage state is highly dependent on the fire and thermal configuration. This is due to the different heating rates of the cross-section as a result of different fire models and, most importantly, different fire protection (Figure 11b). However, after transformation from the time domain to the steel temperature domain, it appears that the attainment of the column damage state as a function of the steel temperature does not depend significantly on the configuration, for the five studied cases (Figure 11c). From the five data points, an average value and standard deviation of the steel temperature can be computed for each (thermal) configuration (Figure 11d). The same process has been applied to the beam damage state and the results are also plotted in Figure 11d. The probabilistic values corresponding to the two configurations are very close, validating therefore the critical temperature approach. The slight differences are probably due to the fact that the temperature is not uniform in the sections. However, these differences can be considered insignificant with respect to the level of uncertainty attached to the system parameters.

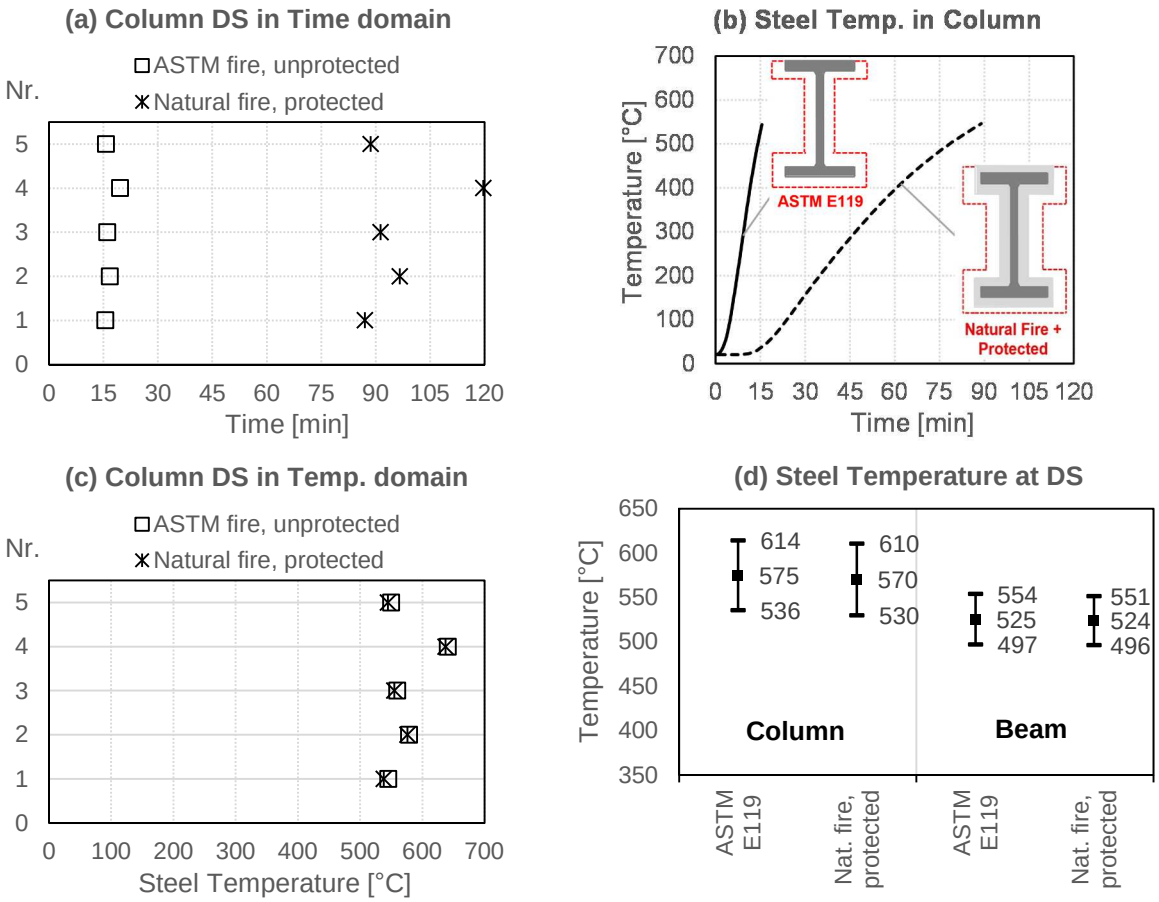

Figure 11. Validation of the critical temperature approach for the studied steel frame building.

As a result, the structural capacity can be characterized in the temperature domain independently of the fire and thermal processes. It is valid as long as no explicit creep term is present in the material model for steel at high temperature, which is the case for instance in the material model from Eurocode. Hence, the stochastic analysis aimed at assessing the probabilistic capacity can be conducted in the temperature domain considering a single fire model. In this study, the ASTM E119 standard fire has been chosen. Similarly, a single set of thermal properties can be adopted and, for reducing the computation time, it is chosen to consider sections with no thermal protection. The resulting probabilistic capacity model can be used for any fire scenario and thermal properties of the structure, within the limits of the conditions listed in Section 2.1.4.

5.4 Structural Capacity Assessment by Stochastic FE Analysis

This section aims at defining the probability density functions (PDF) of the critical temperatures associated with each damage state for the prototype steel frame building. The evolution of temperature in the sections is computed by thermal FE analysis, in a deterministic analysis, considering the standardized ASTM E119 fire. Since this fire is monotonically increasing, any subsequent structural analysis can be run until complete failure, i.e. until attainment of all damage states. Monte Carlo Simulations (MCS) with Latin Hypercube Sampling based on non-linear FE structural analyses are then conducted considering the random

variables of the structural model in Table 2. The analyses are performed using the software SAFIR and the 2D frame model described in Section 3.2.

For each fire location in the building shown in Figure 8, 20 realizations are computed using the probabilistic distributions for gravity loads and steel mechanical properties given in Section 4. Given the eleven fire locations to be studied, a total of 220 simulations is performed. The samples of parameter values are generated using Latin Hypercube Sampling (LHS). Indeed, the number of simulations is limited by the computational effort required to run the FE structural analysis of the building until failure. Use of a selective sampling technique such as LHS is therefore recommended.

Upon heating of the members in the fire-exposed compartment, the strength and stiffness of these members decrease and forces build up due to restraint thermal expansion. The temperature in the members is increased until the two damage states are reached in the structural analysis. For each analysis, the time at which the damage state is reached in the beam and in the column is recorded. The evolution of temperature with time in the sections of the beam and the column is known as a result of the thermal FE analysis. Hence, the time corresponding to the attainment of a damage state can be mapped to the average temperature in the section of the member at this time. As a result, the PDF of capacity relative to each damage state are obtained in terms of critical temperature in the steel section, see Figure 12.

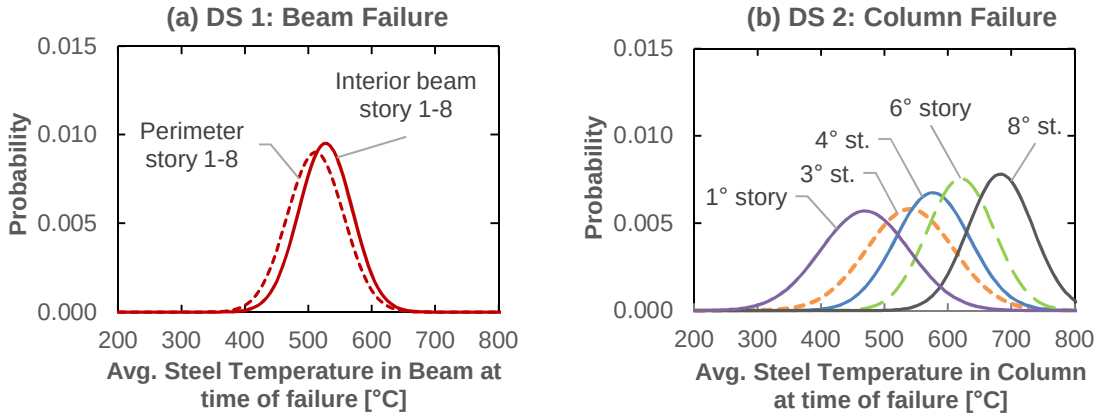

Figure 12. Probability density functions of the damage state in the beam (a) and in the column (b), for different fire locations.

The capacities are assumed to be normally distributed. The normal assumption has been also adopted previously for fire resistance [30]. This assumption is a simplification for the purpose of this example. For a more accurate assessment of the distribution, a larger number of realizations in LHS (e.g. in the order of 100) can be employed, but this raises challenges in terms of computational time when nonlinear FEM is to be used. This paper demonstrates the methodology for deriving fragility functions for fire. However, for obtaining fragility functions to be used in practice, a larger number of realizations is recommended. In future works, the possibility to use simplified models will be investigated to characterize the capacity. These models offer the advantage of being much more computationally efficient than FEM, which makes them more suitable for MCS. The expected loss in accuracy of simplified versus FE

models has to be considered against the gain in probability distribution assessment in a cost-benefit analysis.

Regarding the beam damage state, the PDF's of capacity for a fire in an interior bay are identical for stories 1 to 8, because the beam section type and the applied gravity loads are identical (Table 1) and, as the beams are statically determined, no bending moment is transmitted from the columns to the beams. However, the beam capacity differs slightly in case of fire in a perimeter bay, compared with an interior bay. This is probably due to the different level of lateral restraint, which affects the thermal expansion in the steel beam and therefore the cracking process in the concrete slab. A lower level of lateral restraint (perimeter bay) allows for a larger thermal expansion of the steel beam and the latter causes the cracking of the concrete part of the composite section.

The capacity associated with the column damage state is higher in the upper stories. For this building, lower gravity loads lead to lower utilization ratios in the upper stories even though the cross-sections are smaller than in the lower stories. These lower utilization ratios lead to higher critical temperatures. On the other hand, for the column of the first story, the buckling length is also much higher than for the other columns, which causes buckling failure in this column at relatively low temperature.

6. Demand Assessment by Fire and Heat Transfer Analysis

The next step consists in assessing the demand placed on the structure. For the considered steel building, this demand corresponds to a maximum steel temperature reached in the sections of the structural members. Therefore the analyses carried on in this section aim at deriving the distribution functions of the maximum steel temperature, based on fire modeling and heat transfer analysis.

First, the evolution of temperature in the compartment must be predicted based on a fire model. Selection of the fire model is an important step in the fragility analysis, as the influence of this model on the demand is considerable. Several models for natural fires in compartments have been proposed in the literature and in standard codes, e.g. the parametric fire of Eurocode 1 [27]. For the present example, the model adopted is the natural fire model developed by Quiel and Garlock [31] based on the study of the fire in the One Meridian Plaza (1MP) Building in Philadelphia. It must be noted that the adoption of this simplified model is an assumption to illustrate the methodology developed in this paper. In future studies, the sensitivity of the fragility functions to the fire model will be investigated.

The adopted natural fire curve is dependent on the peak gas temperature and can be scaled accordingly, see Figure 13. To determine the peak gas temperature, the method from Annex A of Eurocode 1991-1-2 is adopted [27], using the values of the parameters given in Section 4 and different levels of fire load between 100 and 2000 MJ/m². The results are given in Table 4.

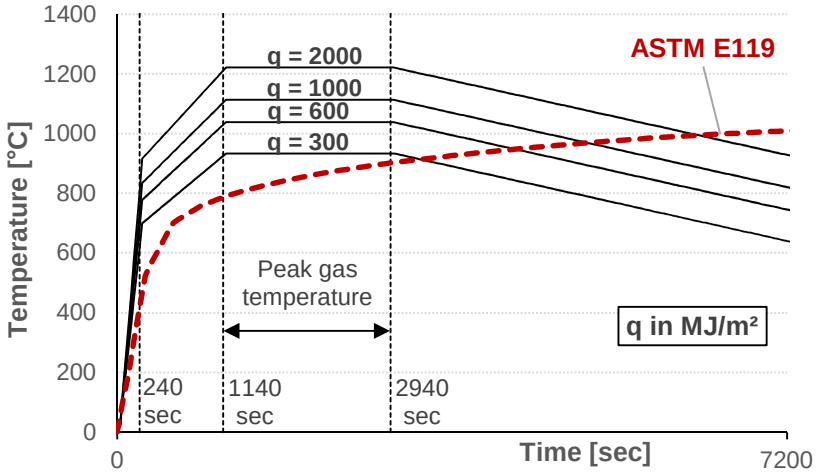

Figure 13. Natural fire model [31] scaled as a function of the peak gas temperature.

Table 4. Peak gas temperature as a function of the fire load.

q [MJ/m²]	100	200	300	400	500	600	700	800	900	1000	1250	1500	2000
$T_{max,gas}$ [°C]	781	872	934	978	1011	1038	1061	1080	1098	1113	1148	1176	1221

Second, the heat transfer analysis must be performed to obtain the temperature evolution in the sections and, hence, the maximum of this temperature. It is assumed that the members are exposed to fire on three sides. The heat transfer analysis can be performed by advanced numerical techniques, such as FE analysis, or using more simple calculation models that are available and efficient to compute the temperature evolution in protected steel sections. Here, the finite difference formula of Eurocode 3 [19] has been adopted, considering its wide acceptance among the structural fire engineering community and its computational efficiency. This formula, also referred to as lumped mass approach, yields the uniform temperature in the cross-section of a steel member at each time step and it can be used for insulated and bare steel members. In this study, for a given structural cross-section and fire load, Monte Carlo Simulations are conducted using the Eurocode formula and varying the thermal properties of the insulation material (thickness and conductivity) as shown in Table 2. For each fire load level, 1000 realizations are computed. The process is then repeated for different levels of fire loads, yielding the distribution of maximum temperature in the steel section corresponding to each fire load level, see Figure 14 for the column of floors 3 and 4. The result is presented in the form of the complementary cumulative distribution function of the maximum steel temperature.

The same methodology is applied to each different cross-section type, i.e. 5 times for the column and 2 times for the beam (see Table 1 for section sizes).

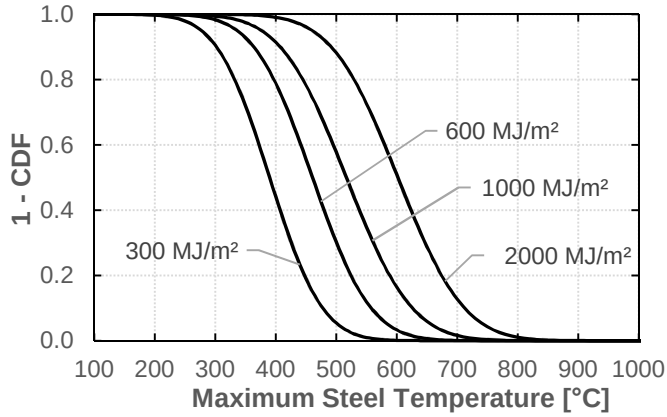

Figure 14. Distribution of max. steel temperature in the column W14x82 (3rd-4th floor) for different levels of fire load, considering variability in SFRM thickness and thermal properties.

7. Fragility Functions

7.1 Derivation for one location

The probability distributions for capacity and demand obtained in Sections 5 and 6 allow for deriving analytical fragility functions for the building. The methodology to derive the fragility function corresponding to a given damage state (e.g. the column damage state) and a given fire location (e.g. the compartment in the second bay of the fourth floor) is illustrated hereafter. The same methodology applies to the other fire locations and damage states.

For the column located in a compartment of the 4th floor, the PDF of capacity and the complementary CDF's of demand have been plotted in Figure 15. The different curves for demand correspond to different levels of fire load. For a given fire load, the conditional probability of failure can be computed using Eq. 1, i.e., by convolution of the PDF of capacity and the complementary CDF of demand corresponding to this fire load. Repeating the operation for each fire load level yields several points relating the fire load level and the conditional probability of failure, see Figure 16. The fragility curve for the beam damage state is also represented in Figure 16.

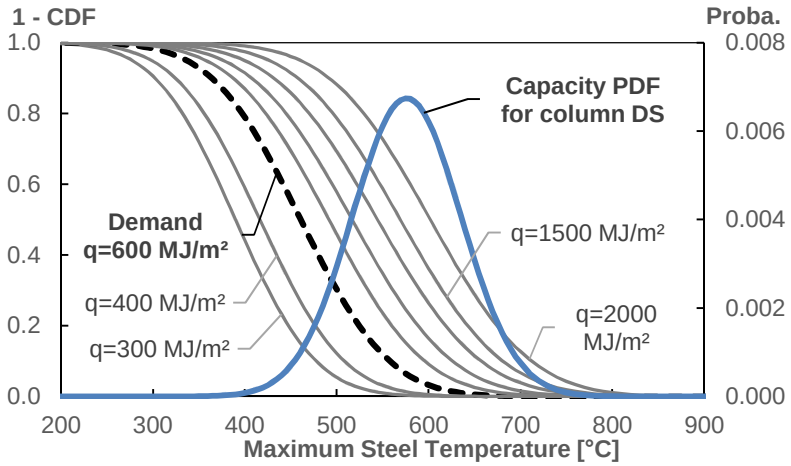

Figure 15. The fragility points are obtained by convolution of PDF of damage state and complementary CDF of demand (here, for the W14x82 column on the 4th floor).

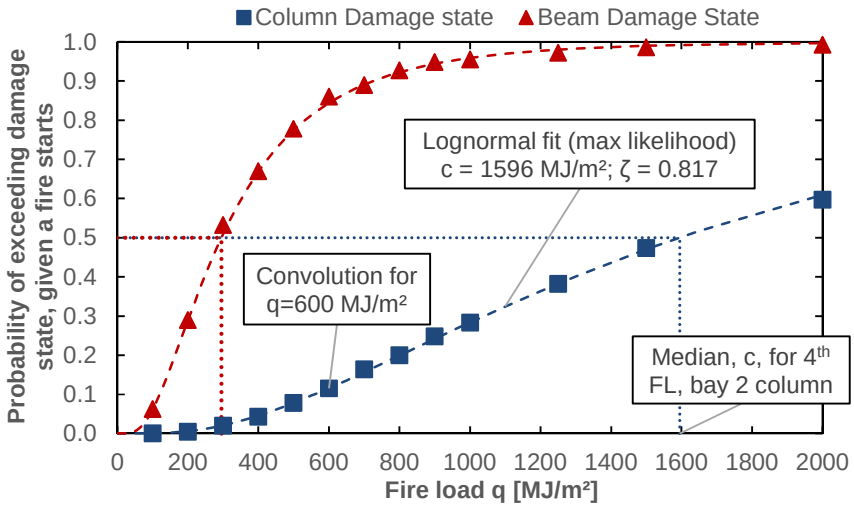

Figure 16. Fragility curves for the beam damage state and the column damage state, conditional to the occurrence of a fire in the 2nd bay of the 4th floor.

The fragility function for a specific state of damage $F(\cdot)$ is assumed to be a lognormal function in the form of:

$$F(q) = \Phi\left[\frac{ln(q/c)}{\zeta}\right] \quad \text{Eq. (2)}$$

In this equation, q is the fire load (MJ/m²) that characterizes the fire and $\Phi[\cdot]$ is the standardized normal distribution function. The two parameters c and ζ characterize the fragility function; they must be determined to maximize the best fit with the data points resulting from the analysis. This fit is performed using the maximum likelihood function:

$$L = \prod_{i=1}^{N}[F(q_i)]^{x_i}[1 - F(q_i)]^{1-x_i} \quad \text{Eq. (3)}$$

In the latter equation, q_i and x_i are the fire loads and the corresponding probabilities of failure obtained by convolution (i.e. for the column, q_i and x_i are the coordinates of the square dots in the plot of Figure 16). N is the total number of points obtained by convolution, for a specific damage state and fire location. The two parameters c and ζ are computed by maximization of L [32]. For the column DS fragility curve plotted in Figure 16, the parameters c and ζ are found equal to 1596 MJ/m² and 0.817, respectively.

The same process is applied for deriving the fragility functions relative to the other damage states and fire compartment locations.

7.2 Combined fragility functions

At this stage, fragility functions associated with the beam and the column damage states have been constructed for each different compartment fire location in the building. It resulted in 9 different fragility functions associated with the column damage state (one at each story) and 4 different fragility functions associated with the beam damage state (2 section sizes, interior and perimeter each). In view of the process of fire disaster evaluation of a community of buildings, a single fragility function per damage state should be used to represent a family of buildings (Figure 1).

For the prototype multi-compartment steel building, the fragility functions analytically developed for each compartment fire location can be combined in order to obtain one combined fragility function per damage state representing the overall building vulnerability. The objective of this section is to propose a methodology to merge the column DS fragility functions corresponding to different compartment fire locations into one single column DS fragility function for the entire building (and similarly for the beam DS fragility function). This methodology is illustrated in the Flowchart 2 (Figure 5) and it is explained here below in three steps. Note that, in this work, the possibility of having a fire extend to several compartments has not been considered.

7.2.1 Step 1: Conditional probability of fire in each story

The first step consists in evaluating the conditional probability for a fire to arise in a specified story, given a fire occurs in the building. This conditional probability is noted $P_{fi,story}|H_{fi}$, in which H_{fi} denotes the probability of having a structurally significant fire in the building per year. The formula of Eq. (4) is used to predict the annual probability P_{fi} for a severe fire able to endanger the structural stability to occur in a compartment with a surface area of A_{fi} (in m²). This formula is the one used for the development of the design values for the fire load densities prescribed in Eurocode [27].

$$P_{fi} = p_{1,EN} \cdot p_{2,EN} \cdot p_{3,EN} \cdot p_{4,EN} \cdot A_{fi} \qquad \text{Eq. (4)}$$

The term $p_{1,EN}$ is the probability of having a fire to start and grow to a severe fire in the compartment, per m² of floor and per year, including the effect of occupants and standard public fire brigade. Additional reduction factors are then applied to this annual frequency to account for active fire protection measures that limit the probability for a fire growth to severe fire. The factor $p_{2,EN}$ considers the effect of the fire brigade type and the time between alarm and firemen intervention. The factor $p_{3,EN}$ takes into account the effect of automatic fire detection and automatic transmission of the alarm. Finally, the factor $p_{4,EN}$ takes into account the effect of sprinkler.

The assumed area of each compartment of the prototype building is 55.7 m² (600 ft²). For illustration of the methodology, a series of assumption are made for estimating the probability and reduction factors in Eq. (4), but of course the developed methodology is not dependent on these particular assumptions and other values could be used. As illustrated in Table 5, it is assumed that the stories 1-7 of the prototype building are for office occupancy, whereas stories 8-9 are dwelling. Between 10 and 20 minutes are required between alarm and the intervention of a professional fire brigade. All fire compartments are assumed to be equipped with automatic fire detection by smoke, but no sprinkler protection system [33].

Table 5. Calculation of the conditional probabilities of fires in a specified story, $P_{fi,story}|H_{fi}$. The intermediate annual probabilities P_{fi} and $P_{fi,story}$ are calculated using Eq. (4) [27] [33].

Story	Use	$p_{1,EN}$	$p_{2,EN}$	$p_{3,EN}$	$p_{4,EN}$	by compartment		by story		$P_{fi,story}\|H_{fi}$
		10^{-7}/m²yr				A_{fi} [m²]	P_{fi} 10^{-7}/year	$A_{fi,story}$ [m²]	$P_{fi,story}$ 10^{-5}/year	
9	Dwelling	7	0.1	0.0625	1.0	55.7	2.44	2090	0.91	0.200
8	Dwelling	7	0.1	0.0625	1.0	55.7	2.44	2090	0.91	0.200
7	Office	3	0.1	0.0625	1.0	55.7	1.04	2090	0.39	0.086
6	Office	3	0.1	0.0625	1.0	55.7	1.04	2090	0.39	0.086
5	Office	3	0.1	0.0625	1.0	55.7	1.04	2090	0.39	0.086
4	Office	3	0.1	0.0625	1.0	55.7	1.04	2090	0.39	0.086
3	Office	3	0.1	0.0625	1.0	55.7	1.04	2090	0.39	0.086
2	Office	3	0.1	0.0625	1.0	55.7	1.04	2090	0.39	0.086
1	Office	3	0.1	0.0625	1.0	55.7	1.04	2090	0.39	0.086
								18810	H_{fi} = 4.57	1.0

The resulting probabilities of severe (or structurally significant) fire are given in Table 5. The probability of a severe fire in a compartment varies from 1.04 x 10^{-7} to 2.44 x 10^{-7} per year. The building comprises many compartments at each story and the probability of a severe fire for the overall story can be found considering the total surface of the story (see Figure 6); this probability varies from 0.39 x 10^{-5} to 0.91 x 10^{-5}. The annual frequency of a structurally significant fire for the overall building is the sum of $P_{fi,story}$ for all stories, thus equal to H_{fi} = 4.57 x 10^{-5}. The total probability of having a fire in the building is approximated here as the sum of the constituent probabilities in each compartment of the building. As a reminder, this probability represents only severe fires, i.e. the fires that develop and grow to significant fire despite the possible action of sprinklers, occupants, fire brigades, etc. For each story, the conditional probability $P_{fi,story}|H_{fi}$ is equal to $P_{fi,story}$ divided by H_{fi}.

7.2.2 Step 2: Conditional probability of each scenario

The conditional probability associated with each compartment fire location, noted p_i, is defined as the conditional probability for a fire to arise in compartment i, given a structurally significant fire occurs in the building. It is calculated using the event tree of Figure 17. This event tree is based on the conditional probability per story, $P_{fi,story}|H_{fi}$, obtained from Table 5. In addition, it is recognized that the proportion of perimeter bays is 2 out of 5 and the proportion of interior bays is 3 out of 5 and, for a given story, the probability of having a fire is equally distributed between each bay. These considerations lead to the definition of the conditional probability for a fire to arise in a specified bay (interior or perimeter) given a fire occurs in the building, $P_{fi,bay}|H_{fi}$, which equals 0.4 for a perimeter bay and 0.6 for an interior bay. Applying these probabilities to the branches of the event tree eventually gives the conditional probabilities p_i for each fire location. For instance, the conditional probability associated to an interior bay of the 9th story is found equal to 0.120, meaning that, if a fire occurs in the building, there is a 12% likelihood that this fire will be in an interior bay at the 9th story.

For a given damage state, as the individual fragility functions correspond to different fire locations, the conditional probabilities p_i are in fact the probabilities with which one individual fragility function will be chosen at random from the combined population of fragility functions. These p_i are thus required to "weigh" each individual function against the others in the process of derivation of the combined fragility function.

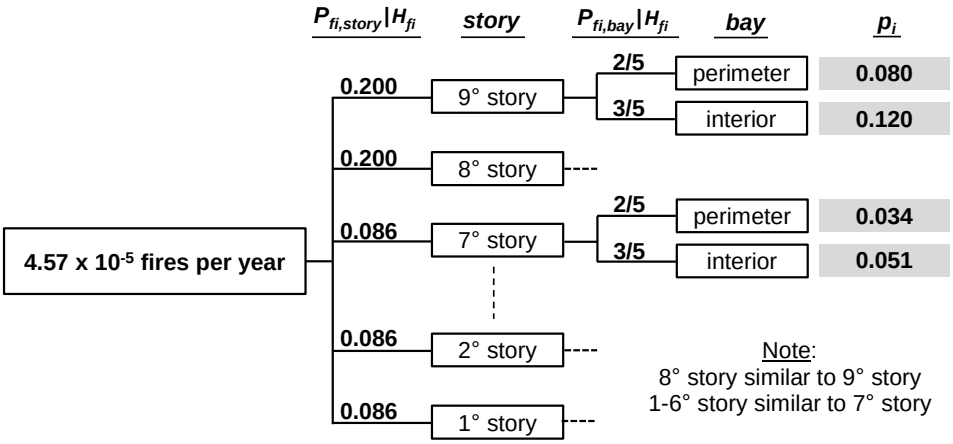

Figure 17. Event tree for the conditional probabilities p_i associated with each fire location.

7.2.3 Step 3: Parameters of the combined fragility functions

In the third step (see Figure 5), the combined fragility functions can be constructed from the individual fragility functions, using the parameters of the individual fragility functions (median and standard deviation) and the probabilities p_i. The mathematical framework for development of combined fragility functions from individual fragility functions constructed for structures with similar structural attributes is adopted from Shinozuka et al. [32].

The combined fragility function $F_c(\cdot)$ representing the overall building vulnerability can be assumed as lognormal according to the following equation:

$$F_c(q) = \Phi\left[\frac{ln(q)-\bar{\alpha}}{\zeta_c}\right] \quad \text{Eq. (5)}$$

In the latter, the parameters $\bar{\alpha}$ and ζ_c that characterize the combined function are estimated from the parameters of the individual fragility functions.

The mean of the combined lognormal distribution is calculated as $\bar{\alpha} = \ln q_c$, with q_c given by Eq. (6). In the latter, n is the number of "nominally identical but statistically different" fragility functions, c_i is the median associated with each individual fragility function (see Eq. 2 and Figure 16), and p_i is the probability with which a scenario i will be chosen at random from the combined population corresponding to each scenario. This probability p_i corresponds in this case to the conditional probability for a fire to arise in compartment i, given a fire occurs in the building (Figure 17).

$$q_c = \prod_{i=1}^{n} c_i^{p_i} \quad \text{Eq. (6)}$$

The standard deviation of the combined lognormal distribution, ζ_c, is calculated using Eq. (7). In the later, **P** is the vector of the probabilities p_i, **Z** is the vector of the variances ζ_i^2

associated with each individual fragility function (see Eq. 2), **A** is the vector of the expected values $\alpha_i = \ln c_i$, and **Q** is the matrix given by Eq. 8. The reader is referred to [32] for more comprehensive information about the combination process.

$$\zeta_c^2 = \mathbf{P^T Z} + \mathbf{A^T Q A} \quad \text{Eq. (7)}$$

$$\mathbf{Q} = \begin{bmatrix} p_1(1-p_1) & \cdots & -p_1 p_n \\ \vdots & \ddots & \vdots \\ -p_n p_1 & \cdots & p_n(1-p_n) \end{bmatrix} \quad \text{Eq. (8)}$$

Table 6 summarizes the parameters for the individual fragility functions and the conditional probabilities p_i (from Figure 17) associated to each fire location. For the column damage state, the individual fragility functions depend on the story but do not depend on the bay (perimeter or interior). Therefore, the probabilities p_i have been summed per story.

Table 6. Parameters for the combined fragility functions, calculated from the individual fragility parameters and the conditional probabilities, for the column and the beam DS.

		Column			**Beam**		
Story	**Bay**	c_i **[MJ/m²]**	ζ_i	p_i	c_i **[MJ/m²]**	ζ_i	p_i
9	Perimeter	1725	0.845	0.08+0.12	156	0.737	0.080
	Interior			=0.200	142	0.720	0.120
8	Perimeter	2040	0.795	0.08+0.12	259	0.712	0.080
	Interior			=0.200	295	0.701	0.120
7	Perimeter	1288	0.788	0.034+0.51	259	0.712	0.034
	Interior			=0.086	295	0.701	0.051
6	Perimeter	1619	0.798	0.034+0.51	259	0.712	0.034
	Interior			=0.086	295	0.701	0.051
5	Perimeter	1137	0.838	0.034+0.51	259	0.712	0.034
	Interior			=0.086	295	0.701	0.051
4	Perimeter	1596*	0.817*	0.034+0.51	259	0.712	0.034
	Interior			=0.086	295*	0.701	0.051
3	Perimeter	1199	0.886	0.034+0.51	259	0.712	0.034
	Interior			=0.086	295	0.701	0.051
2	Perimeter	1897	0.817	0.034+0.51	259	0.712	0.034
	Interior			=0.086	295	0.701	0.051
1	Perimeter	771	0.945	0.034+0.51	259	0.712	0.034
	Interior			=0.086	295	0.701	0.051
Combined		q_c **= 1513**	ζ_c **= 0.880**	**1.0**	q_c **= 246**	ζ_c **= 0.757**	**1.0**

* see Figure 16

The variation between stories of the median fire load c_i associated with each column fragility function is mainly due to the variation in the demand over capacity ratio at ambient

temperature. Indeed, a same column type is used for two consecutive stories (Table 1) although the demand (gravity load) is different. This explains the transition in c_i between two consecutive stories.

The parameters of the combined fragility functions for the prototype steel building can be calculated using Eq. 6-8. The parameters q_c and ζ_c of the combined fragility functions are given at the bottom of Table 6, for the two damage states.

7.2.4 Fragility functions for the entire building

The lognormal fragility curves for the entire building, constructed using the combined parameters of Table 6, are shown in Figure 18, for the column damage state (a) and the beam damage state (b). The individual fragility curves are also plotted. The combined curves fall within the range of the individual curves; they represent a "weighed average" of the vulnerability of the building to fire.

The combined fragility curves associated to the two damage states for the overall building are plotted in Figure 19. Based on the average value of the fire load that is expected in the building, the multi-story building fragility curves yield the probability of exceeding each damage state, conditional to the occurrence of a structurally significant fire in one compartment of the building. In this probabilistic model, it is thus not necessary to assess in which particular compartment the fire develops. Instead, the model provides a probabilistic assessment of the degree of damage for a building similar to this prototype building in which a compartment fire develops somewhere and, despite the active fire protection measures, reaches a point where it is able to endanger the structural stability. The effect of the passive fire protection (SFRM) is incorporated in the fragility curves.

For instance, assuming that the fire load is equal to 600 MJ/m² (in average) in the building, Figure 19 shows that the probability of exceeding the beam damage state (DS1) is 88% and the probability of exceeding the column damage state (DS2) is 15%.

For the sake of discussion, it is assumed here that the beam damage state is always reached prior to the column damage state or, in terms of probability, $P(\text{DS1}|\text{DS2})=1$. The assumption is the most likely scenario given the archetype configuration (geometric, member sizes, structural system, etc.) and the distribution functions for the random parameters. Here, adopting this assumption, the probability of exceeding the damage state in the beam (DS1) but without collapse of the column can be calculated as $P(\text{DS1})-P(\text{DS2})=73\%$. The latter situation can be referred to as a "moderate damage" in the building due to fire, considering the structural repair that would be required subsequent to the fire. On the other hand, in case of column failure, the structure is said to experience "severe damage". The probability of not reaching any of the two considered structural damage state is obtained as the complement of the probability of DS1, i.e. 12% for a fire load of 600 MJ/m².

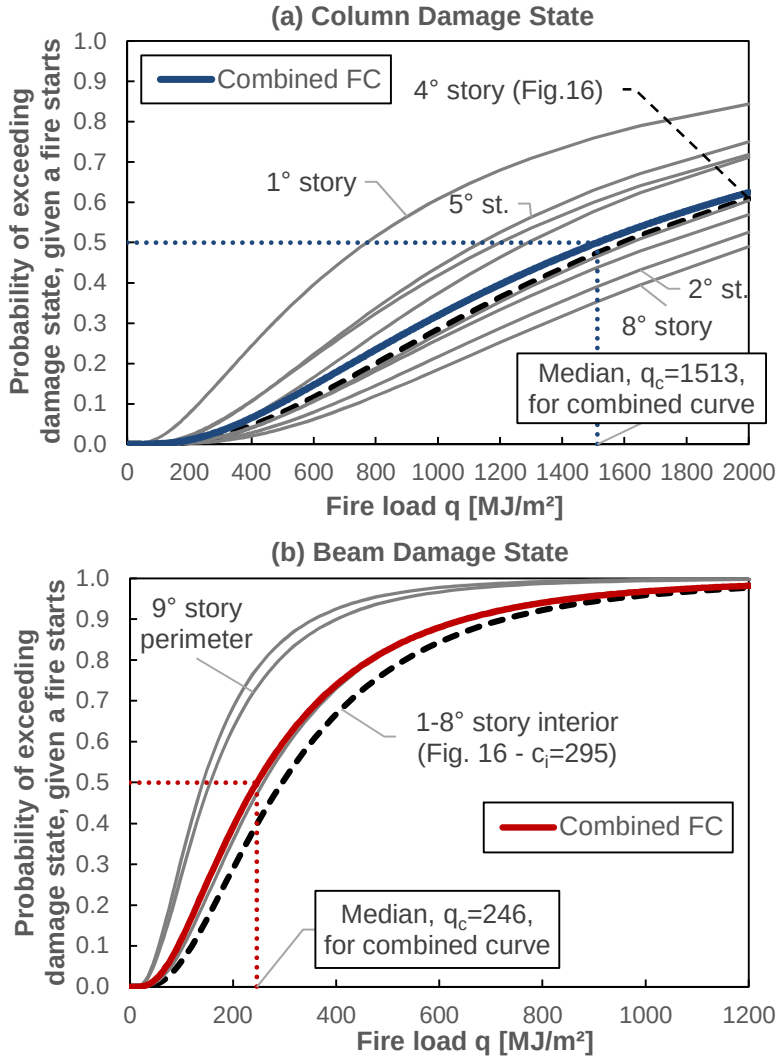

Figure 18. Combined fragility curve associated to the column damage state (a) and the beam damage state (b), obtained from the combination of the fragility curves for each fire location.

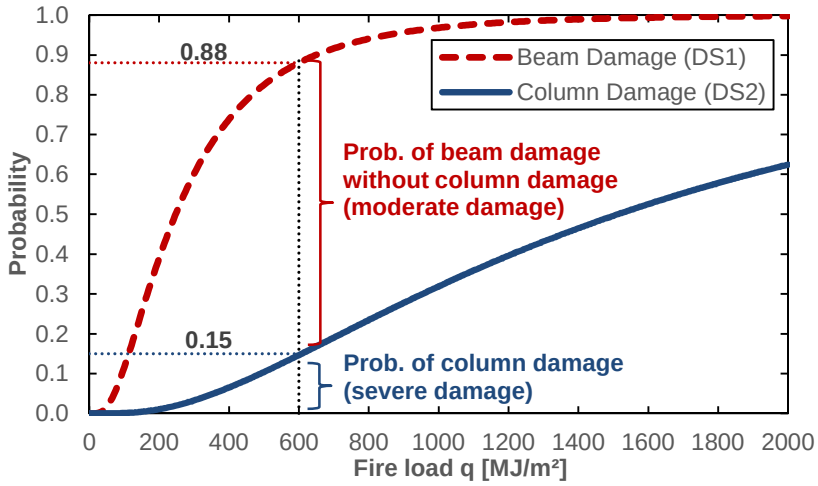

Figure 19. Combined fragility curves for the prototype nine-story steel frame building, representing the overall vulnerability of the building.

The fire load on the x-axis of the fragility curves graph of Figure 19 is an unfactored fire load. The user should evaluate the fire load actually present in the building, without applying any factor based on the occupancy, risk of fire activation, etc. Indeed, the purpose of these factors in the design codes such as Eurocode [27] is to weigh the fire load to get a design value that implicitly includes the probability of a structurally significant fire to occur. However, the fragility curves give conditional probabilities of failure, given that a structurally significant fire has occurred in a compartment. Based on the methodology used to derive the fragility functions, the fire load should therefore not include a second time any factor related to the probability of a fire to occur.

Figure 19 shows that the vulnerability of the building to fire is significant, although the steel structure is protected with SFRM. The probabilities of reaching the structural damage states in fire increase quickly with the fire load density, especially for the beam. The median of the beam damage state fragility function is 246 MJ/m², which is not a high value compared to the fire load densities typically found in office buildings [2]. However, it is important to note that these are conditional probabilities. The probability of a structurally significant fire in a building is low: it was previously estimated in the order of 5×10^{-5} per year for the prototype building. A significant conditional probability of fire damage does therefore not necessarily imply a low safety factor relative to fire hazard (notably, if active fire protection measures are implemented to decrease the annual frequency of significant fires).

9. Conclusion

This study proposes a novel methodology for developing fire fragility functions for an entire steel building. The proposed framework accounts for the different sources of uncertainties that affect the vulnerability of a steel building to fire, both at the material scale and at the building scale. The probability distributions of structural capacity and demand placed on the members are assessed separately in the temperature domain and then convolved to yield the conditional probability of failure for discrete values of the fire load (i.e. the fragility points). The fragility functions are then obtained by fitting these fragility points. In addition, a probabilistic framework based on event tree analysis is introduced for taking into account the different possible fire locations in a multi-compartment building and their associated likelihood. The method incorporates the effect of different occupancy or active fire protection measures on the distribution of likelihood between compartments.

The developed fragility functions can be applied in a probabilistic fire disaster assessment of a community of buildings. First, the probability of structurally significant fire in a community of buildings is estimated, per year or per accidental event (e.g. following an earthquake). Second, the fragility functions are used to predict the level of structural damage for each individual building subject to a fire as a function of the fire load in this building. These results eventually allow for an estimation of the expected loss due to fire in the community.

Buildings within a community are made of varied structural types and materials. Hence specific fragility functions are needed to characterize the vulnerability of these different types

of buildings to fire. Further works shall focus on the development of reliable and accurate fire fragility functions for different types of structures.

The methodology developed in this work can be applied for constructing analytical fire fragility functions for other typologies of steel structures. One key aspect for steel structures lies in the separation between the thermal and the mechanical problem, taking advantage of the fact that the capacity and demand can be characterized in the temperature domain. This is not necessarily true for other structural materials such as concrete.

Acknowledgments

Thomas Gernay is supported by the Belgian American Educational Foundation, Inc. (BAEF) and the Commission for Educational Exchange between the United States of America, Belgium and Luxembourg (Fulbright). Funding is also provided by Princeton University through "Project X" grant.

References

[1] Iqbal, S., Harichandran, R. S. (2011). Capacity reduction and fire load factors for LRFD of steel columns exposed to fire. *Fire Safety J*, *46*(5), 234–242.

[2] Elhami Khorasani, N., Garlock, M., Gardoni, P. (2014). Fire load: Survey data, recent standards, and probabilistic models for office buildings. *Eng Struct*, *58*(0), 152–165.

[3] Ellingwood, B. R. (2005). Load combination requirements for fire-resistant structural design. *J Fire Prot Eng*, 15(1), 43-61.

[4] Nowak, A.S., Szerszen, M.M. (2003) Calibration of Design Code for Buildings (ACI 318): Part 1-Statistical Models for Resistance, *ACI Struct J*, 100(3), 377-382.

[5] Elhami Khorasani, N., Gardoni, P., Garlock, M. (2015). Probabilistic Fire Analysis: Material Models and Evaluation of Steel Structural Members. *J Struct Eng ASCE*.

[6] Lange, D., Devaney, S., Usmani, A. (2014). An application of the PEER performance based earthquake engineering framework to structures in fire. *Eng Struct*, *66*(0), 100–115.

[7] Nigro, E., Bilotta, A., Asprone, D., Jalayer, F., Prota, A., Manfredi, G. (2014). Probabilistic approach for failure assessment of steel structures in fire by means of plastic limit analysis. *Fire Safety J*, *68*, 16–29.

[8] Guo, Q., Jeffers, A. E. (2014). Finite-Element Reliability Analysis of Structures Subjected to Fire. *J Struct Eng ASCE*.

[9] Eamon, C. D., Jensen, E. (2013). Reliability analysis of reinforced concrete columns exposed to fire. *Fire Safety J*, *62*, 221–229.

[10] Annerel, E., Caspeele, R., Taerwe, L. (2013). Full-Probabilistic Analysis of Concrete Beams During Fire. *Journal of Structural Fire Engineering*, *4*(3), 165–174.

[11] Guo, Q., Shi, K., Jia, Z., & Jeffers, A. (2013). Probabilistic Evaluation of Structural Fire Resistance. *Fire Technol*, *49*(3), 793–811.

[12] Van Coile, R., Caspeele, R., & Taerwe, L. (2014). Reliability-based evaluation of the inherent safety presumptions in common fire safety design. *Eng Struct*, *77*, 181–192.

[13] Karim, K. R., & Yamazaki, F. (2003). A simplified method of constructing fragility curves for highway bridges. *Earthq Eng Struct D*, *32*(10), 1603–1626.

[14] Ji, J., Elnashai, A. S., Kuchma, D. (2007). An analytical framework for seismic fragility analysis of RC high-rise buildings. *Eng Struct*, *29*(12), 3197–3209.

[15] Rota, M., Penna, A., Magenes, G. (2010). A methodology for deriving analytical fragility curves for masonry buildings based on stochastic nonlinear analyses. *Eng Struct*, 32(5), 1312–1323.

[16] Vaidogas, E. R., & Juocevi, V. (2008). Reliability of a timber structure exposed to fire : estimation using fragility function. *Mechanika*, *73*(5), 35–42.

[17] Lee, S., Davidson, R., Ohnishi, N., Scawthorn, C. (2008). Fire Following Earthquake – Reviewing the State-of-the-Art of Modeling. *Earthq Spectra*, 24(4), 933-967.

[18] Davidson, R. (2009). Modeling Postearthquake Fire Ignitions Using Generalized Linear (Mixed) Models. *J Infrastruct Syst*, 15, 351-360.

[19] EC3, *Eurocode 3: Design of steel structures – Part 1-2: General rules – Structural fire design*. EN 1993-1-2, Brussels: CEN, 2005.

[20] Elhami Khorasani, N., Garlock, M., Gardoni, P. (2014). Reliability-based approach for evaluation of buildings under post-earthquake fires. In G.-Q. Li, S.-C. Jiang, S.-W. Chen, V. K. R. Kodur, J. Jiang, & G.-B. Lou (Eds.), *Proc. 8th Int. Conf. Structures in Fire* (pp. 877–886). Shanghai: Tongji University Press.

[21] Agarwal, A., Varma, A.H. (2014). Fire induced progressive collapse of steel building structures: The role of interior gravity columns. *Eng Struct*, *58*, 129-140.

[22] Franssen, J.M. (2005). SAFIR: A thermal/structural program for modeling structures under fire. *Eng J AISC*, *42*(3), 143-158.

[23] Quiel, S. E., & Garlock, M. E. M. (2010). Parameters for Modeling a High Rise Steel Building Frame Subject to Fire. *Journal of Structural Fire Engineering*, 1(2), 115–134.

[24] Gernay, T., Franssen, J. M. (2012). A formulation of the Eurocode 2 concrete model at elevated temperature that includes an explicit term for transient creep. *Fire Safety J*, *51*, 1–9.

[25] Iqbal, S., Harichandran, R. S. (2010). Capacity reduction and fire load factors for design of steel members exposed to fire. *J Struct Eng ASCE*, 1554-1562.

[26] National Fire Protection Association (NFPA). NFPA 557 standard for determination of fire loads for use in structural fire protection design, MA; Ed. 2012.

[27] EC1, *Eurocode 1: Actions on structures – Part 1-2: General actions – Actions on structures exposed to fire*. EN 1991-1-2, Brussels: CEN, 2002.

[28] Drysdale D. An introduction to fire dynamics, 2nd ed. Chichester, UK: Wiley, 1998.

[29] ASTM - American Society for Testing and Materials. ASTME119-00 –Standard Methods of Fire Test of Building Construction and Materials. West Conshohocken, PA, USA, 2007

[30] He, Y. (2013). Probabilistic fire-risk-assessment function and its application in fire resistance design. *Procedia Engineering*, 62, 130-139.

[31] Quiel, S. E., Garlock, M. E. M. (2008). A closed-form analysis of perimeter member behavior in a steel building frame subject to fire. *Eng Struct*, 30(11), 3276–3284.

[32] Shinozuka, M., Member, H., Member, A., Lee, J., Naganuma, T. (2000). Statistical Analysis of Fragility Curves. *J Eng Mech ASCE*, 126(12), 1224–1231.

[33] Vassart, O., Zhao, B., Cajot, L.G., Robert, F., Meyer, U., Frangi, A. *Eurocode: Background & Applications. Structural Fire Design. Worked Examples*. JRC, Luxemburg, 2014.